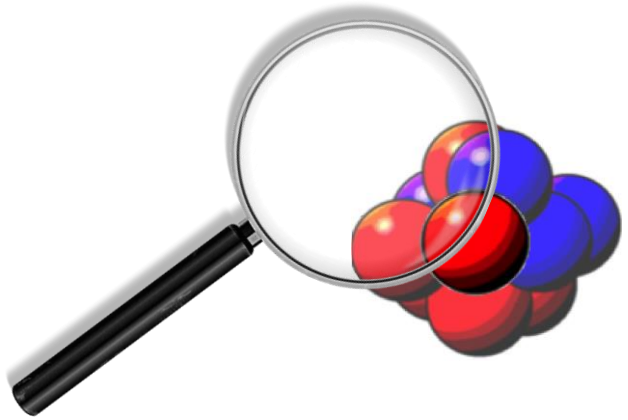

Exclusive Measurement of Single-Proton Strength in Quasi-Elastic $^{12}C(p, 2p)^{11}B$ at High Momentum Transfer

Maria Patsyuk, VBLHEP

JINR PAC63, Jan 26, 2026

First SRC experiment at BM@N in 2018

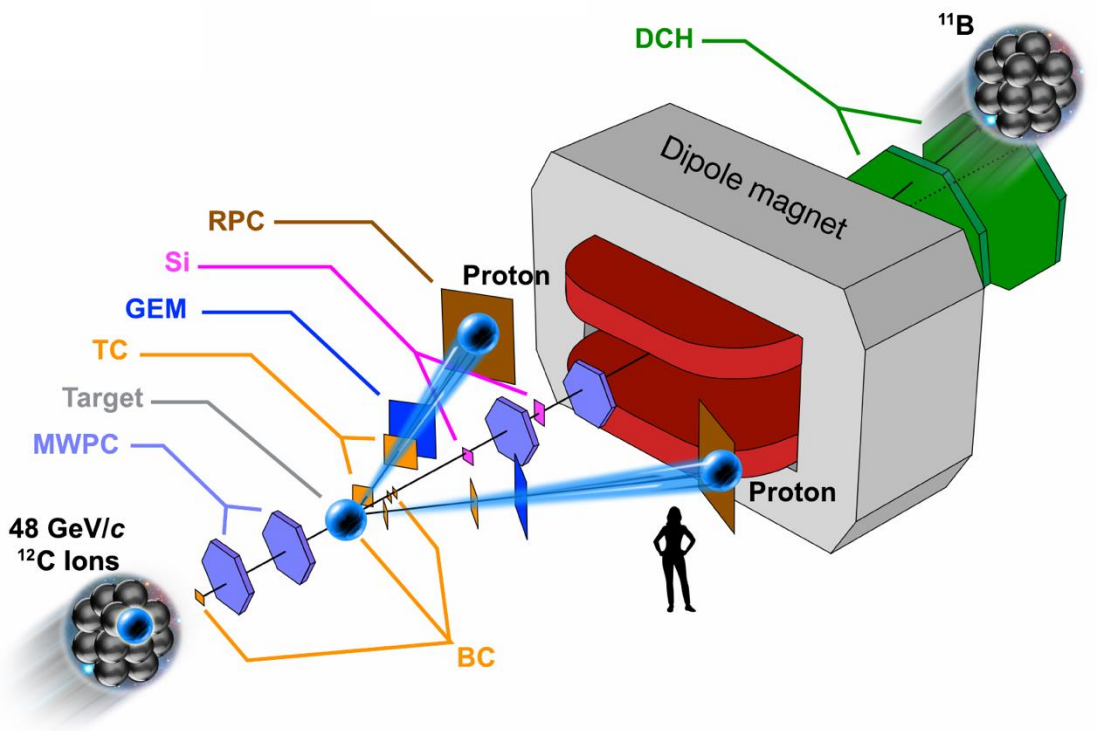

Analysis of QE $^{12}C(p,2p)^{11}B$ established **suppressed rescattering in ISI/FSI**,

but no absolute cross section determined

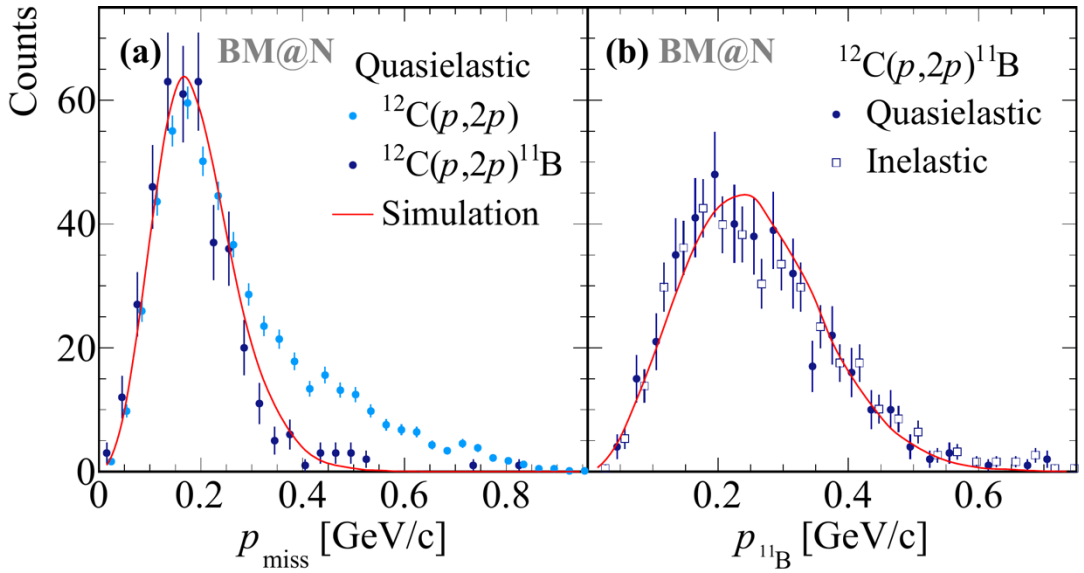

M. Patsyuk et al, (BM@N), Nat. Phys. 17 693 (2021)

Quenched nuclear single-particle strength

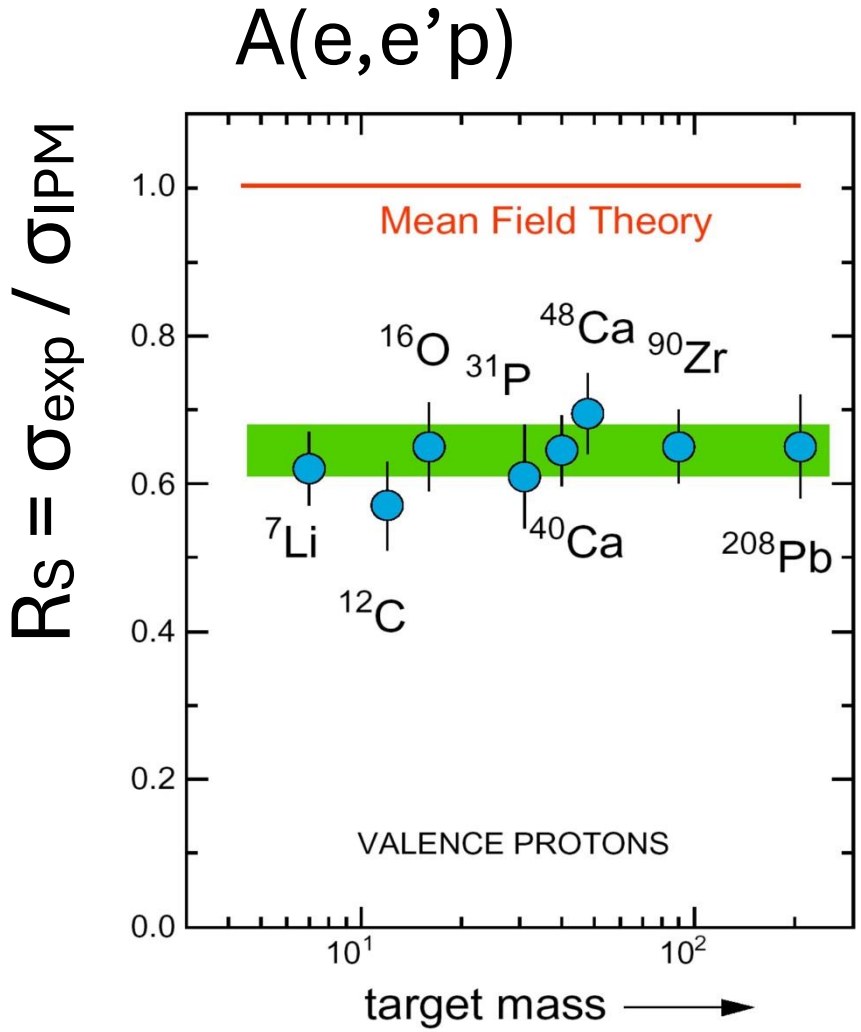

L. Lapikas, NPA 553 (1993)

Quenched nuclear single-particle strength

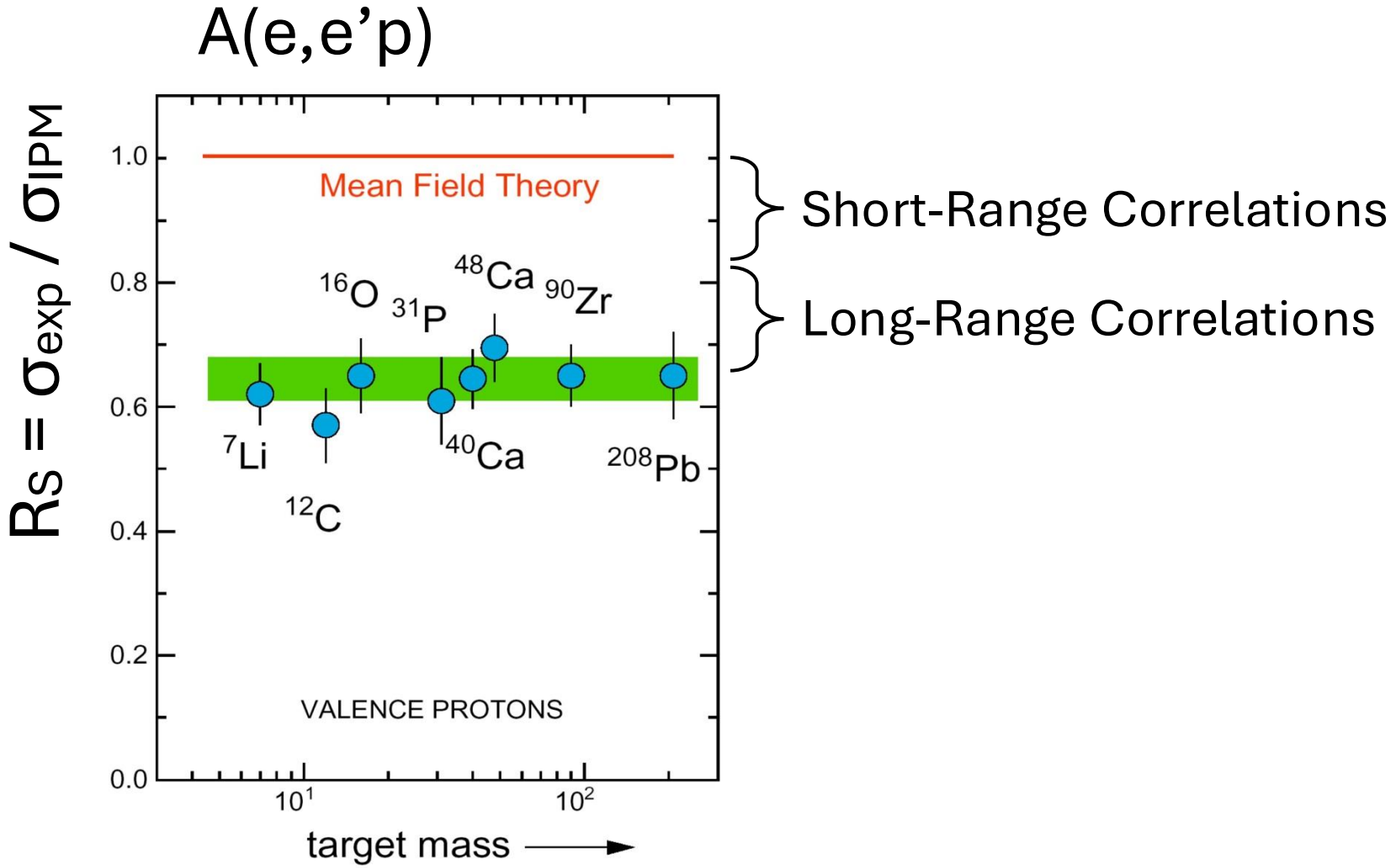

L. Lapikas, NPA 553 (1993)

Quenching observed in transfer reactions

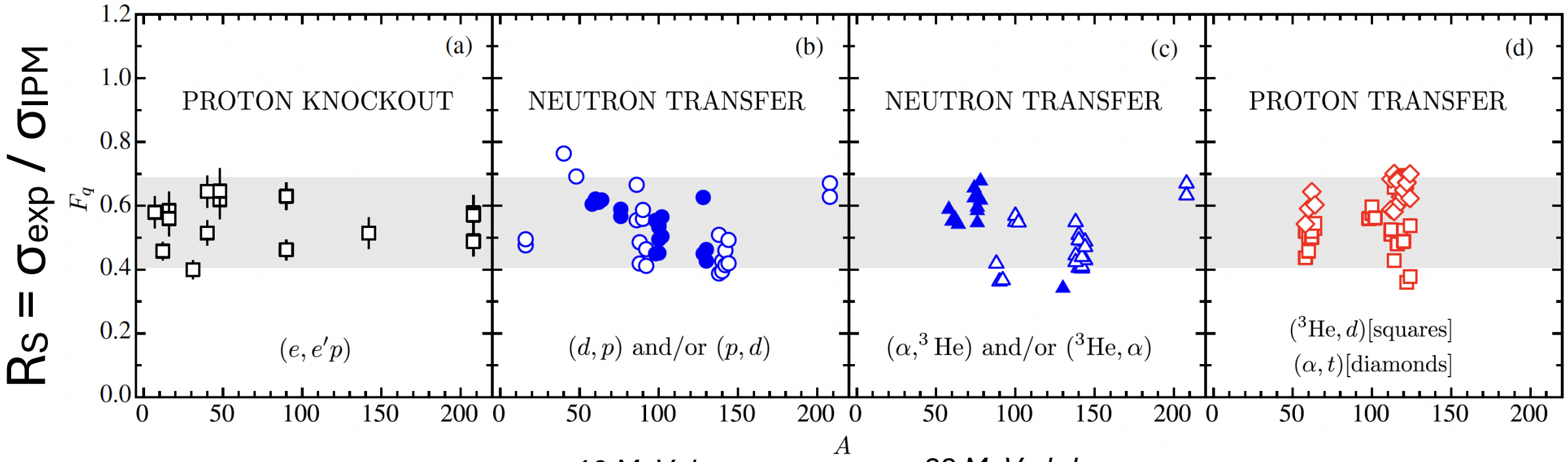

10 MeV d
28 MeV p

38 MeV alpha
25 MeV ^{3}He

Solid symbols – from adding and removing reactions
Open symbols – just adding or just removing

B. P. Kay et al., Phys. Rev. Lett. 111 (2013) 042502

Quenching observed in various reactions

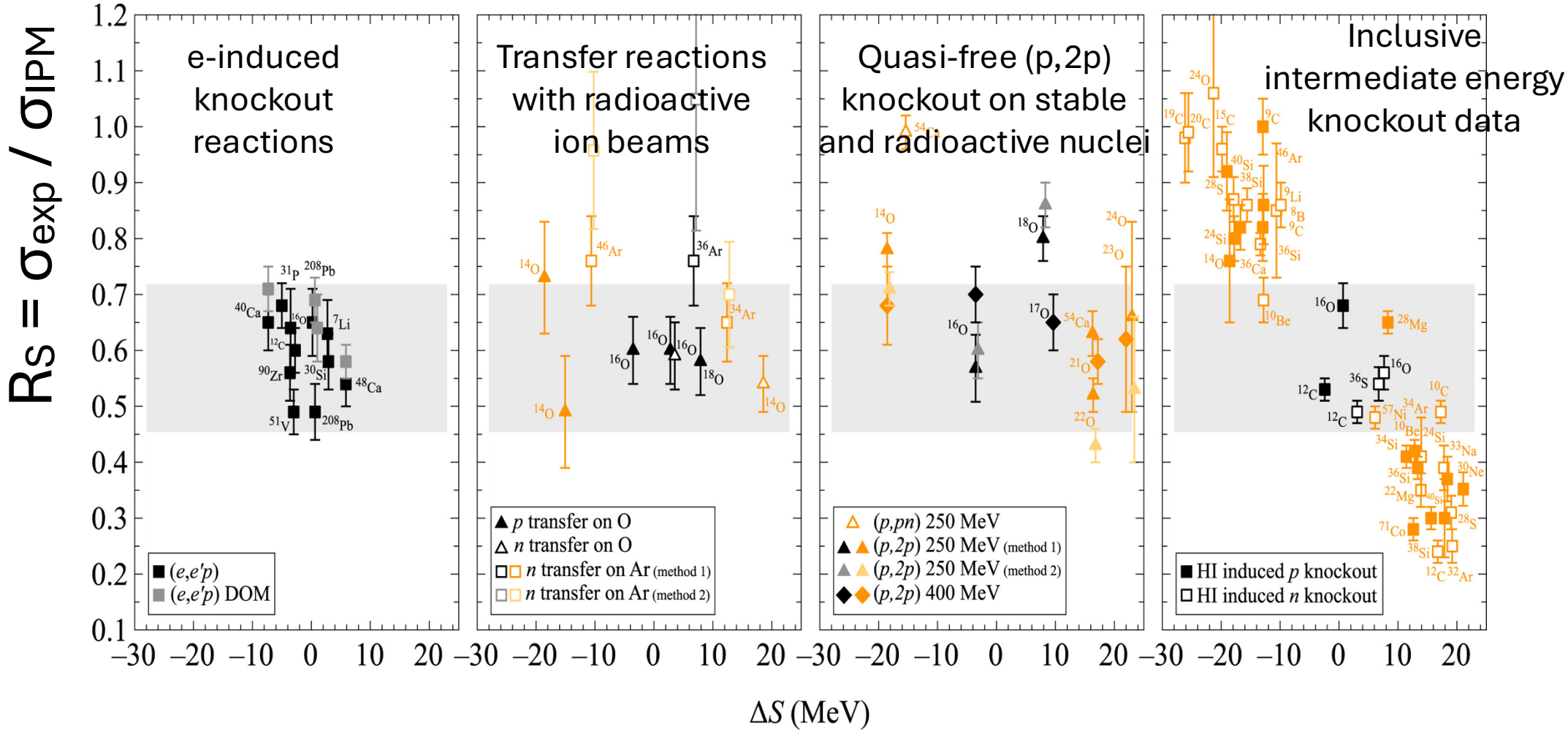

T. Aumann et al., Prog. Part. Nucl. Phys. 118 (2021)

Quenching for ^{12}C from $^{12}C(p,2p)^{11}B$ at 11.38 GeV/c

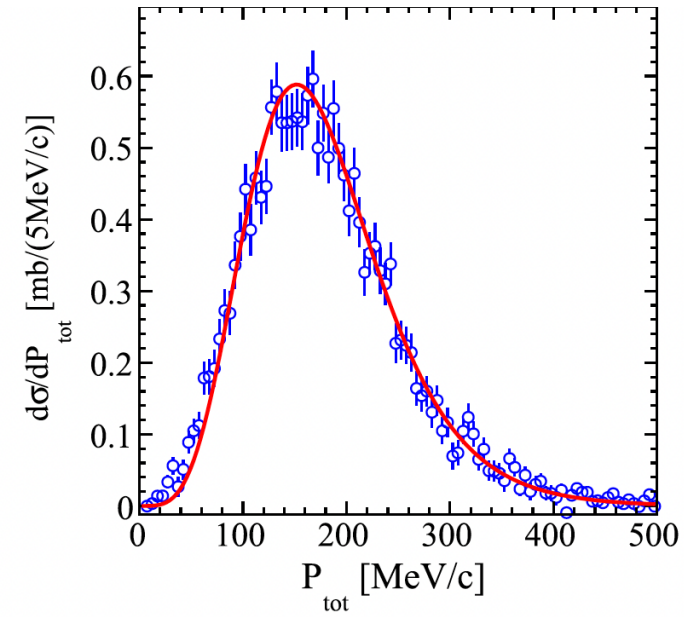

Momentum transfer around 0.37 $(GeV/c)^2$

$$R_s = \frac{\sigma_{exp}}{\sigma_{theory}} = 0.6 \pm 0.07$$

V. Panin et al., Phys. Lett. B 753, 204 (2016)

^{12}C spectroscopic strength: scale dependence?

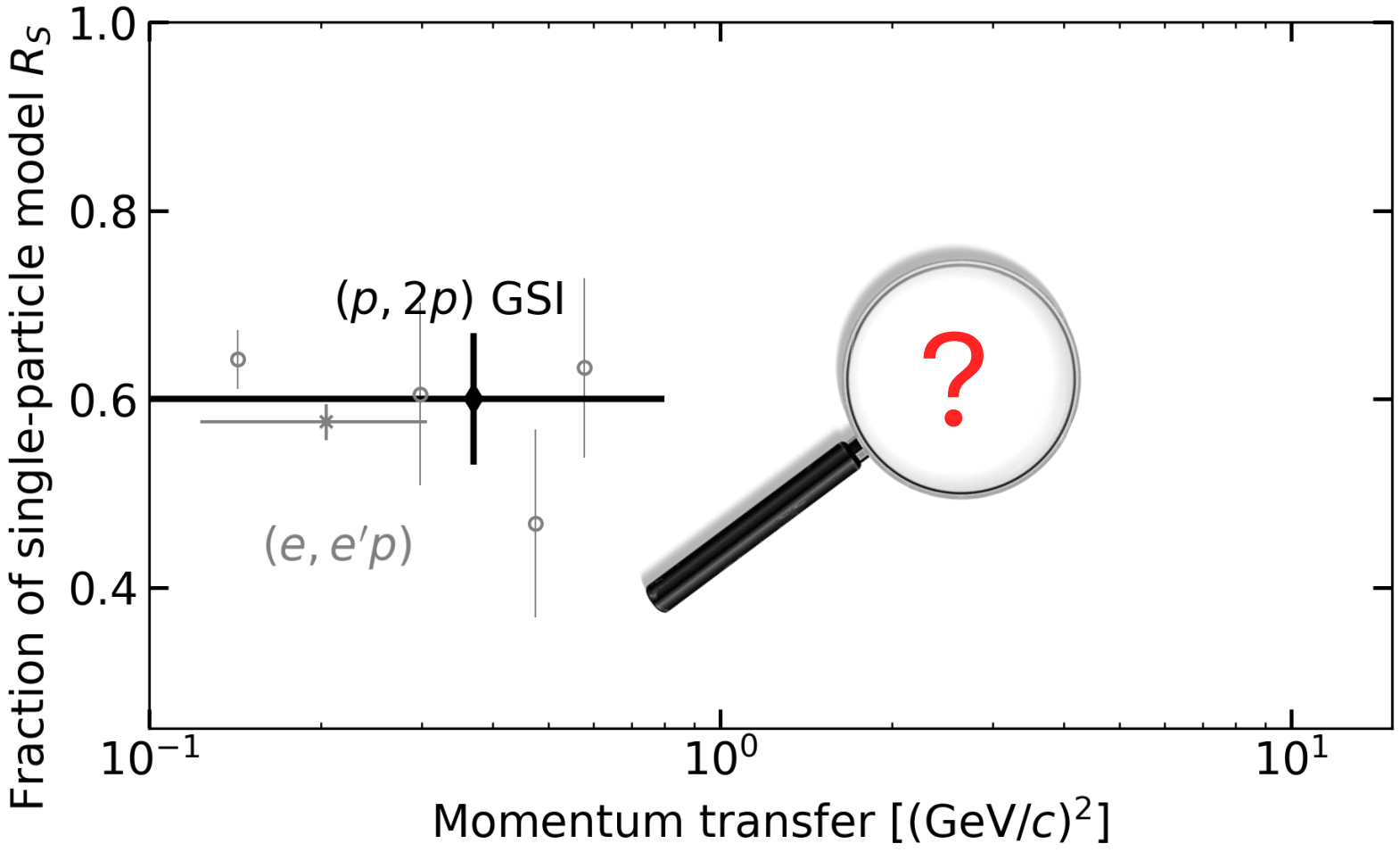

Experiment $^{12}C(p,2p)^{11}B$ at BM@N in 2022

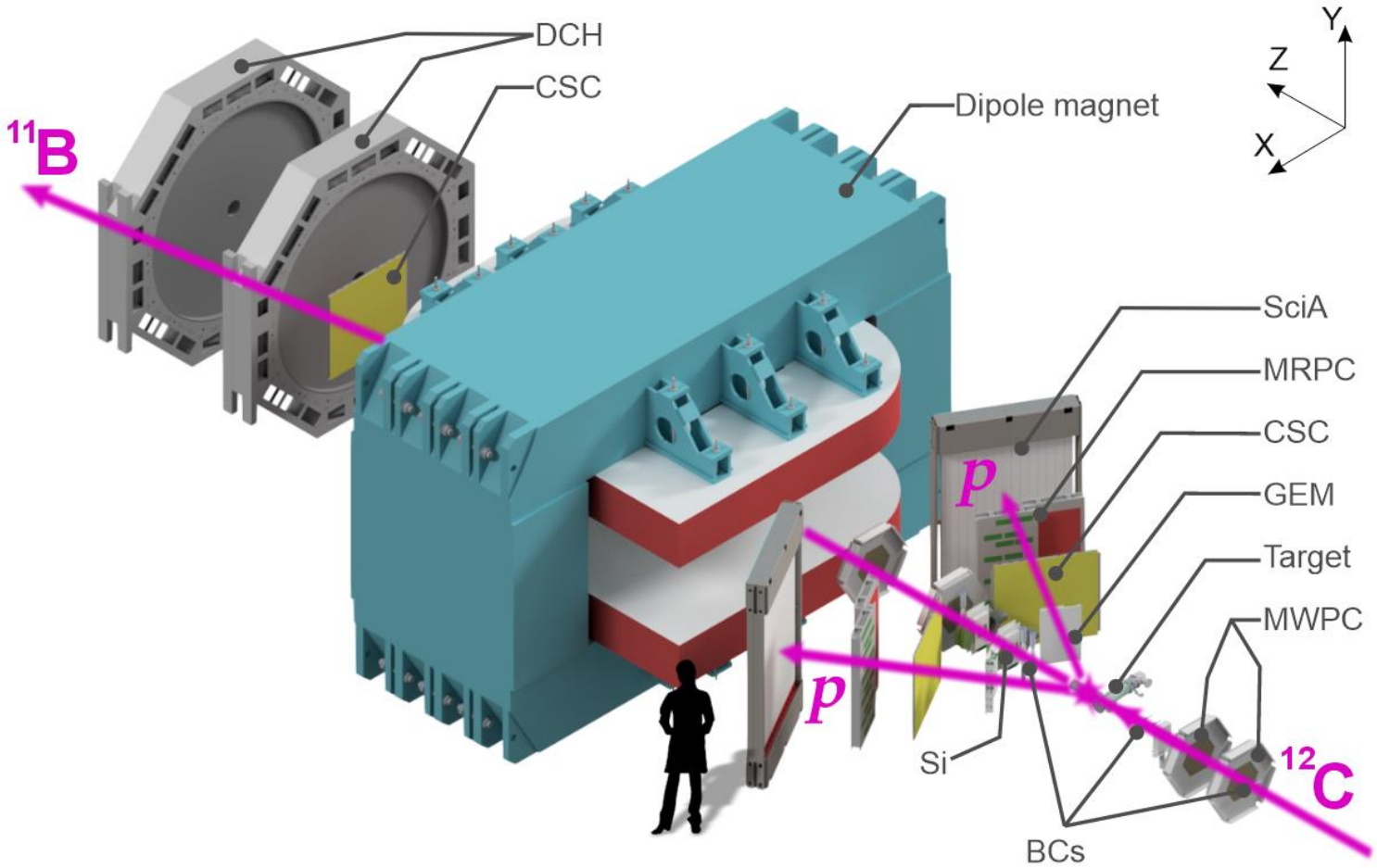

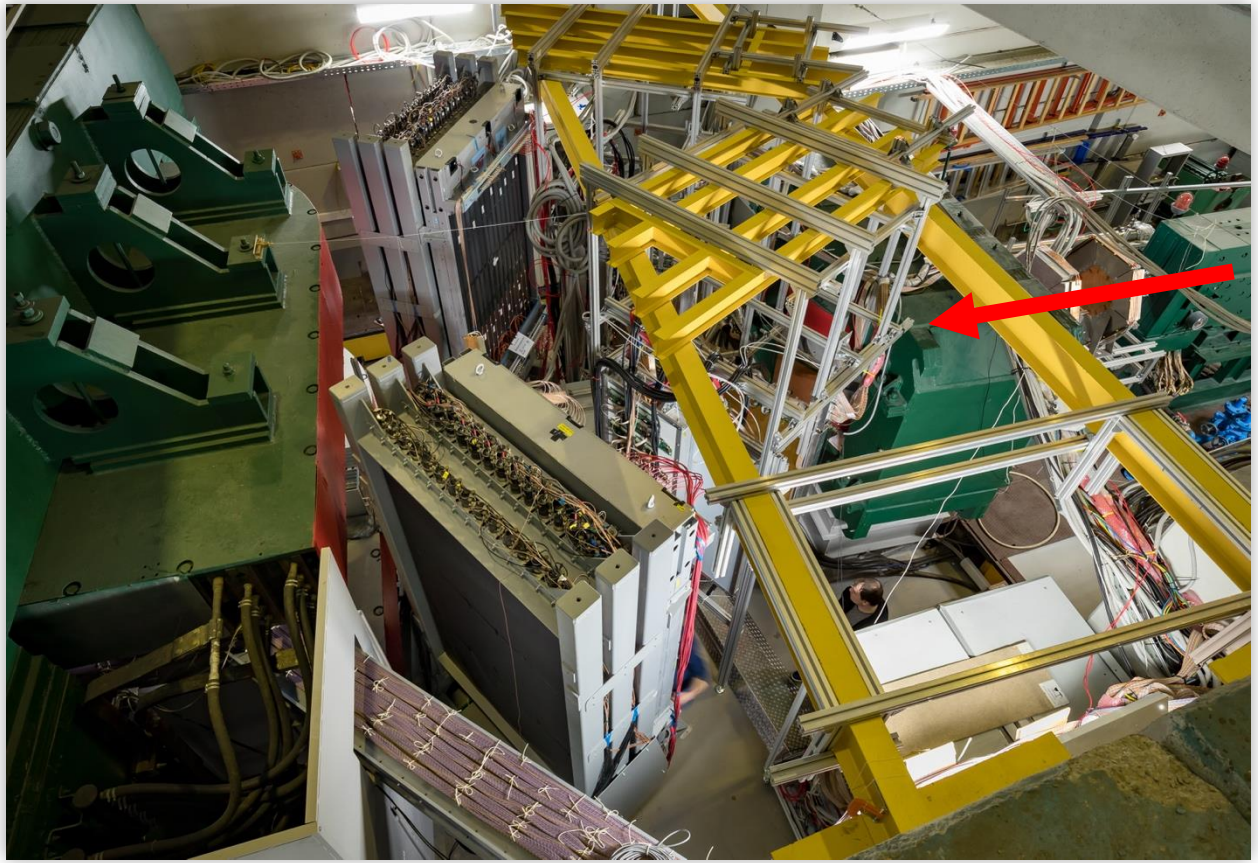



Triggers

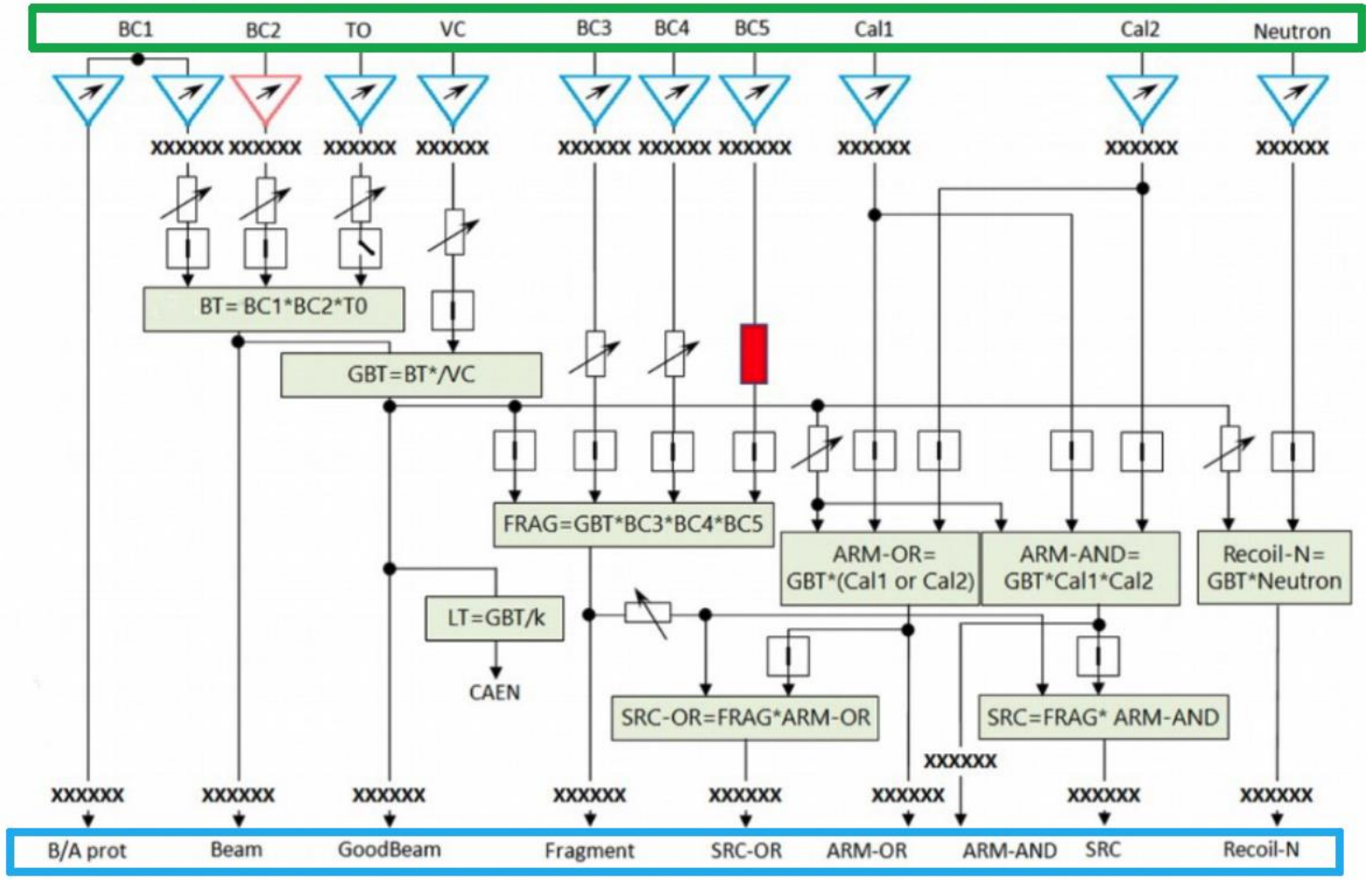

We used 3 triggers:
Beam
Good Beam
ArmAnd

Physics data taking:
ArmAnd + BT/700 + Laser10Hz

Any of 3 triggers can generate a trigger candidate to start the DAQ

Reaction trigger rate 180 Hz at a lifetime ~100%

A list of ”good runs” is defined based on accumulated triggers and constant trigger ratio bwt beam triggers and laser triggers

Beam

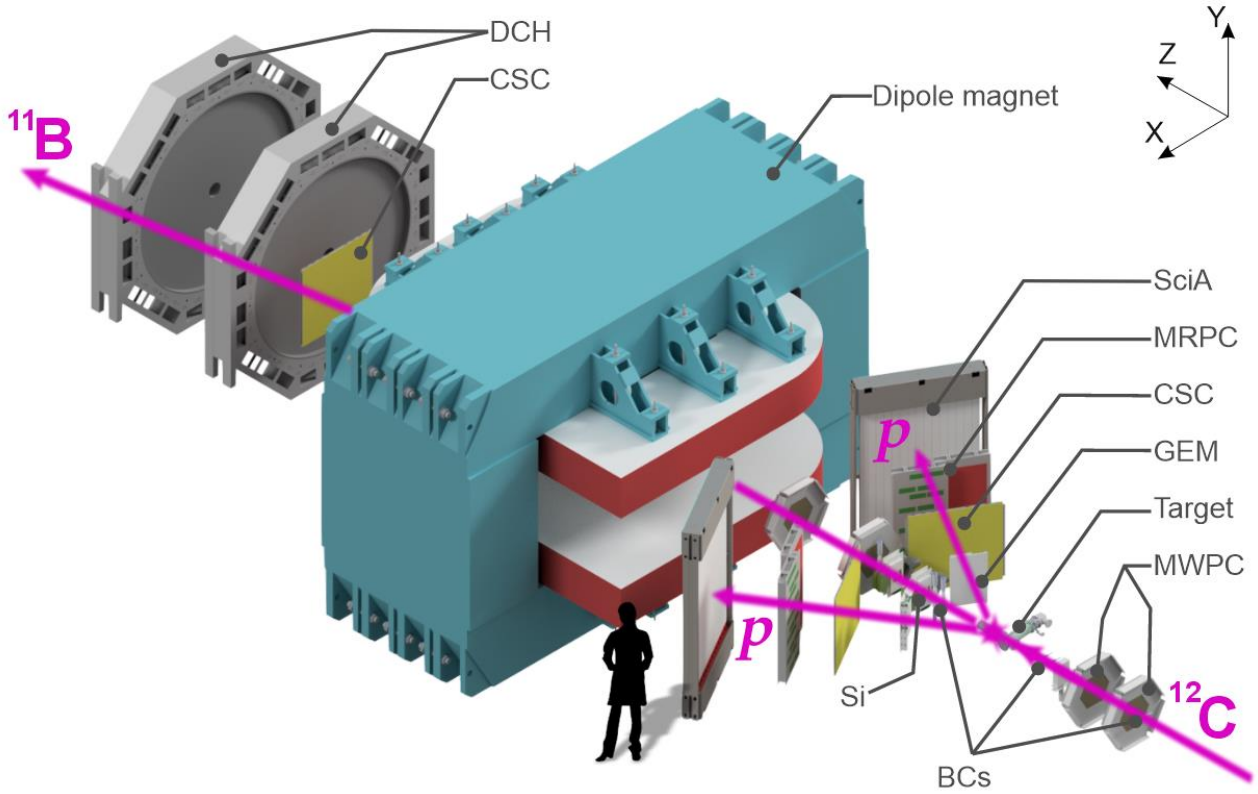

^{12}C from laser source with 100% purity and momentum 3.73 GeV/c/u at the target with dp/p ~ 0.15 %

First physics run using Booster ring

10 s period with spill length of 2-5 s

Average intensity 2.5 x 10^5 ions/s

^{11}B fragment selection ^{12}C(p,2p)^{11}B

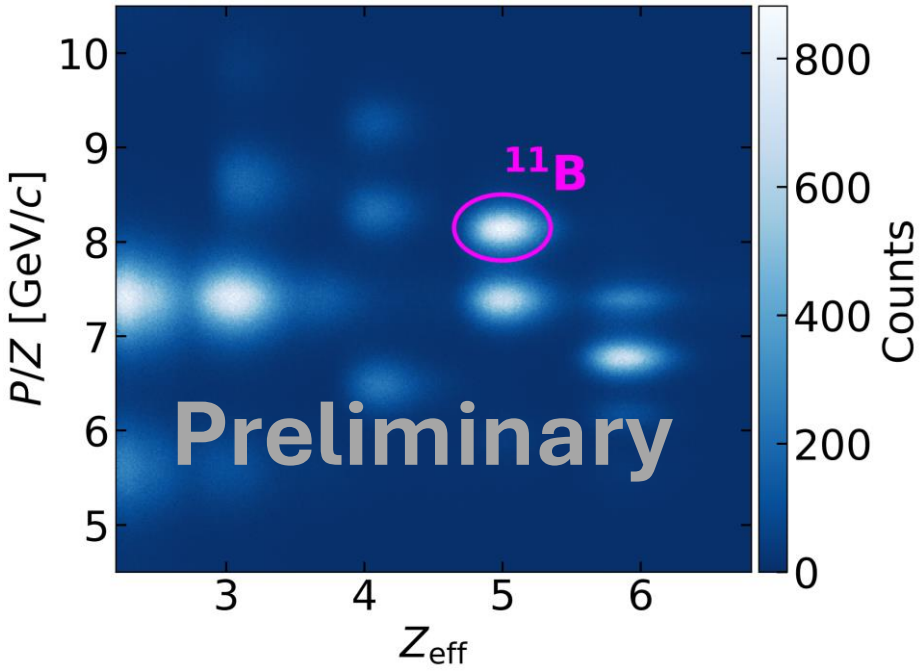

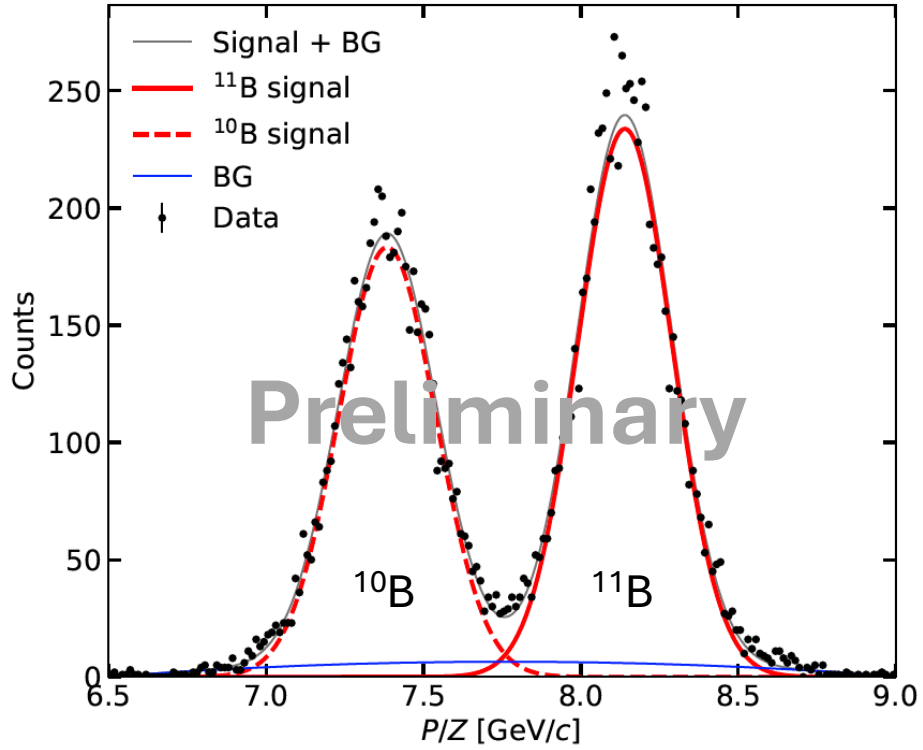

P/Z was estimated using Multi-Dimensional Fit (MDF) method

Seminar on Upstream tracks last week by T. Atovullaev

MDF в нашем случае

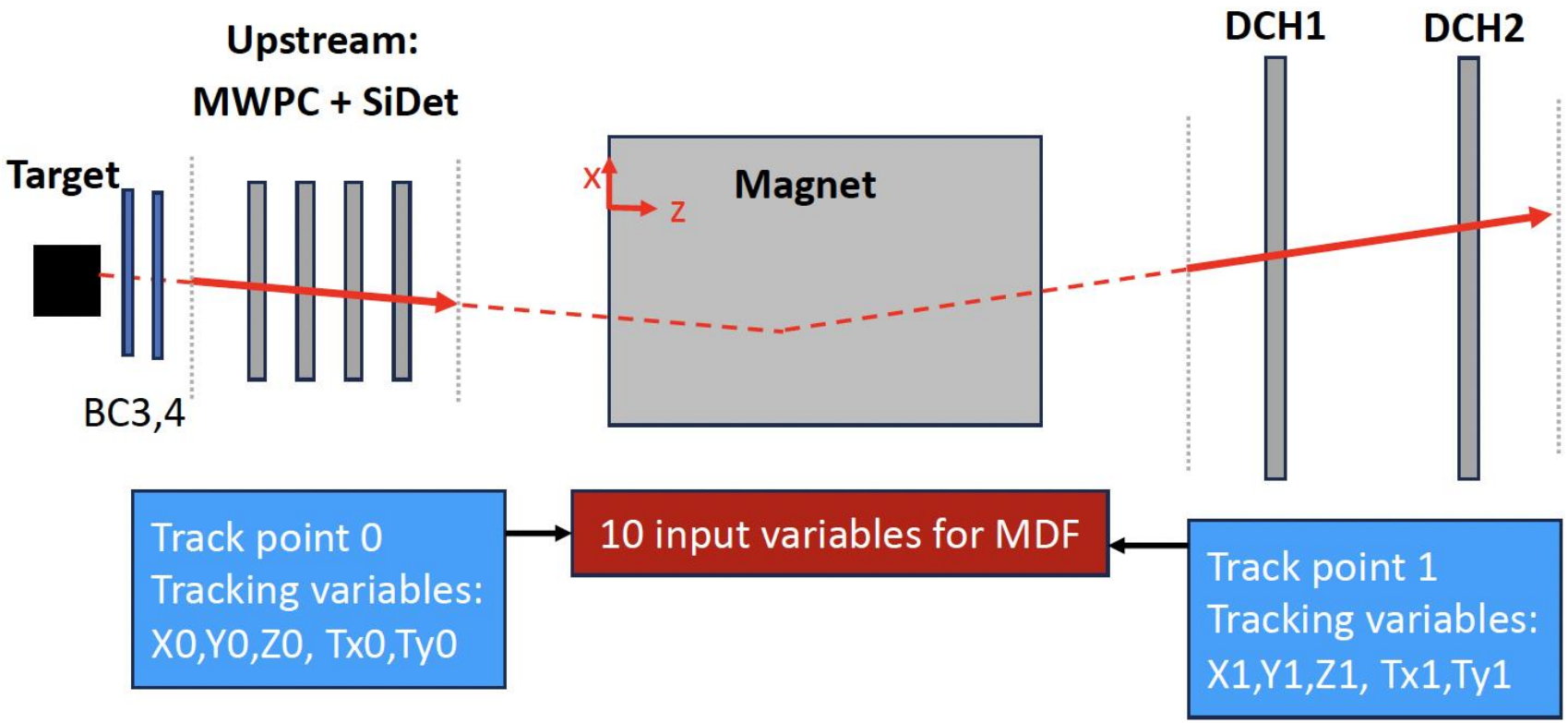

$$\mathbb{P}_{\mathbf{p}}(\mathbf{x_j}) = \sum_{l=1}^{L} c_l \, f_l(\mathbf{x_j})$$

$$S = \sum_{j=1}^{M} (\mathbb{P}_j - \mathbb{P}_p(\boldsymbol{x_j}))^2 \, / \boldsymbol{\sigma_j}^2$$

M - number of events

$\mathbb{P}_{\mathbf{p}}$ это $TX0_{mdf} = f_9$ (X0, Y0, Z0, TY0, X1, Y1, Z1, TX1, TY1) или $P/Z_{mdf} = f_{10}$ (X0, Y0, Z0, TX0, TY0, X1, Y1, Z1, TX1, TY1)

$\boldsymbol{x_j}$ - от 1…10 – параметры трека в одном событии: до магнита (положение X0, Y0, Z0 и тангенсы углов TX0, TY0) и после магнита X1, Y1, Z1, TX1, TY1.

c_l - искомые коэффициенты

$\mathbb{P}_j$ - известные величины $TX0_{mdf}$ и P/Z_{mdf}, полученные из моделирования

Momentum reconstruction with MDF

Step 1:

Simulation

Input:

Wide beam + wide momentum

Unreacted nuclei

Track before magnet

Track after magnet

Known momentum

Output:

P/q (X_0, Y_0, Z_0, Tx_0, Ty_0, X_1, Y_1, Z_1, Tx_1, Ty_1)

$Tx_{\text{before magnet}}$ (X_0, Y_0, Z_0, Ty_0, X_1, Y_1, Z_1, Tx_1, Ty_1)

Step 2:

Momentum reconstruction

Input:

Track before magnet

Track after magnet

Matching conditions (ΔTx, ΔTy < 4 sigma)

Output:

P/q

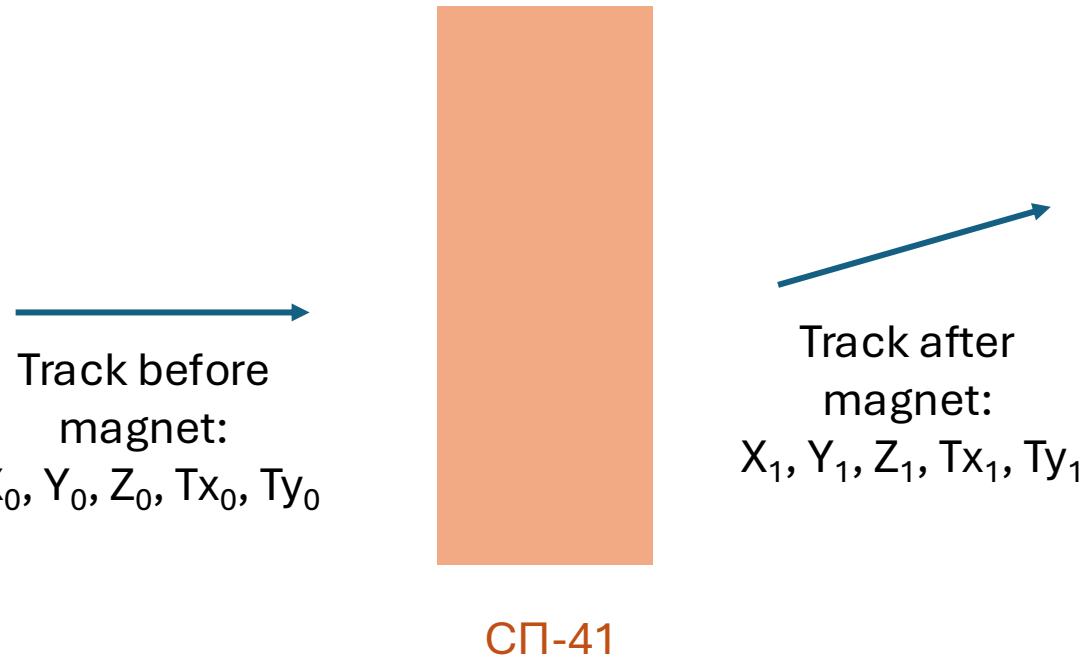

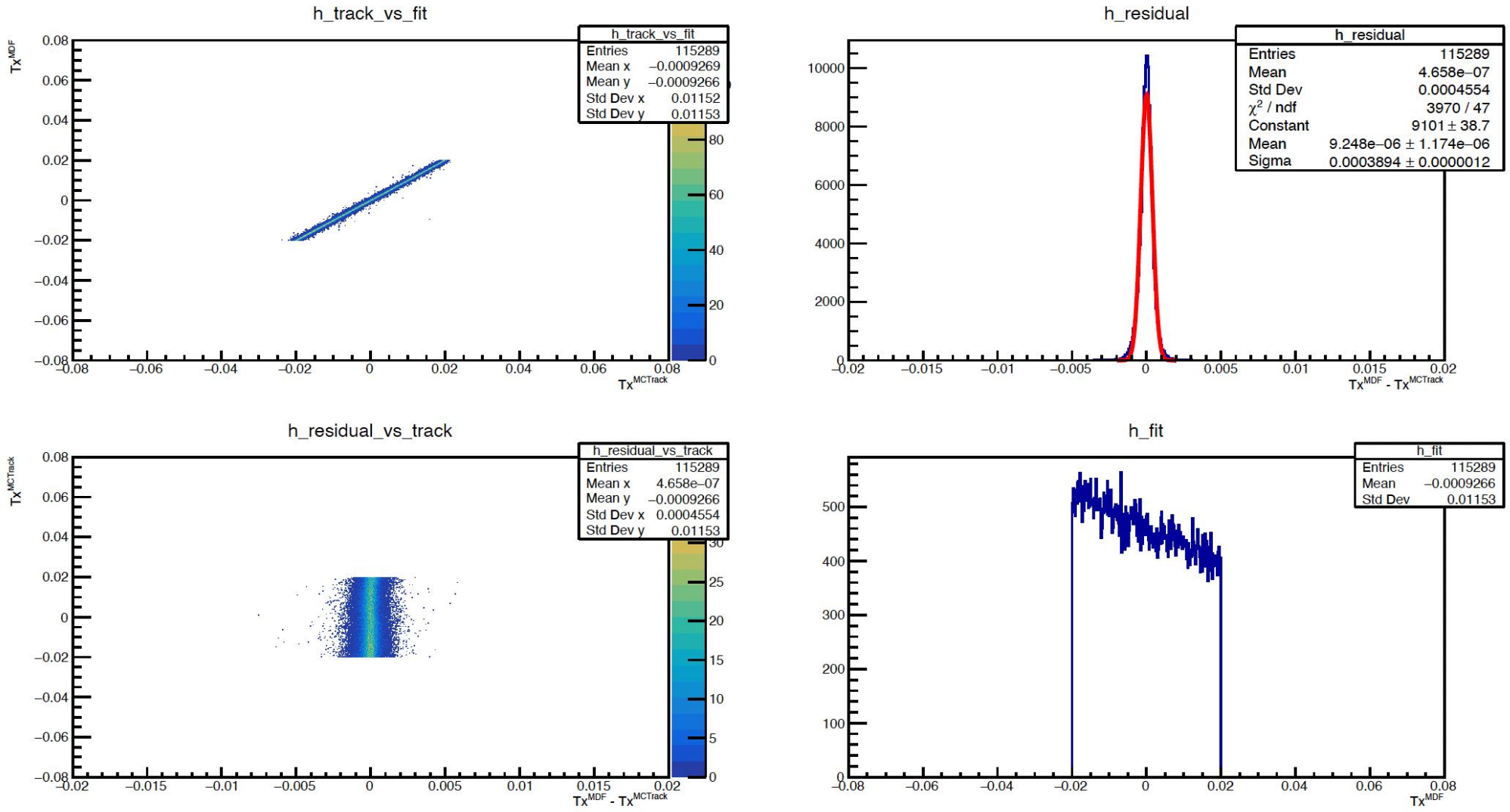

Figure 91: The results of Multi-Dimensional Fit to 300 000 simulated Monte-Carlo tracks of ^{12}C without detector resolutions. $TX0_{track}$ is the true value (simulation input) and $TX0_{mdf}$ is the corresponding value obtained from the Multi-Dimensional Fit.

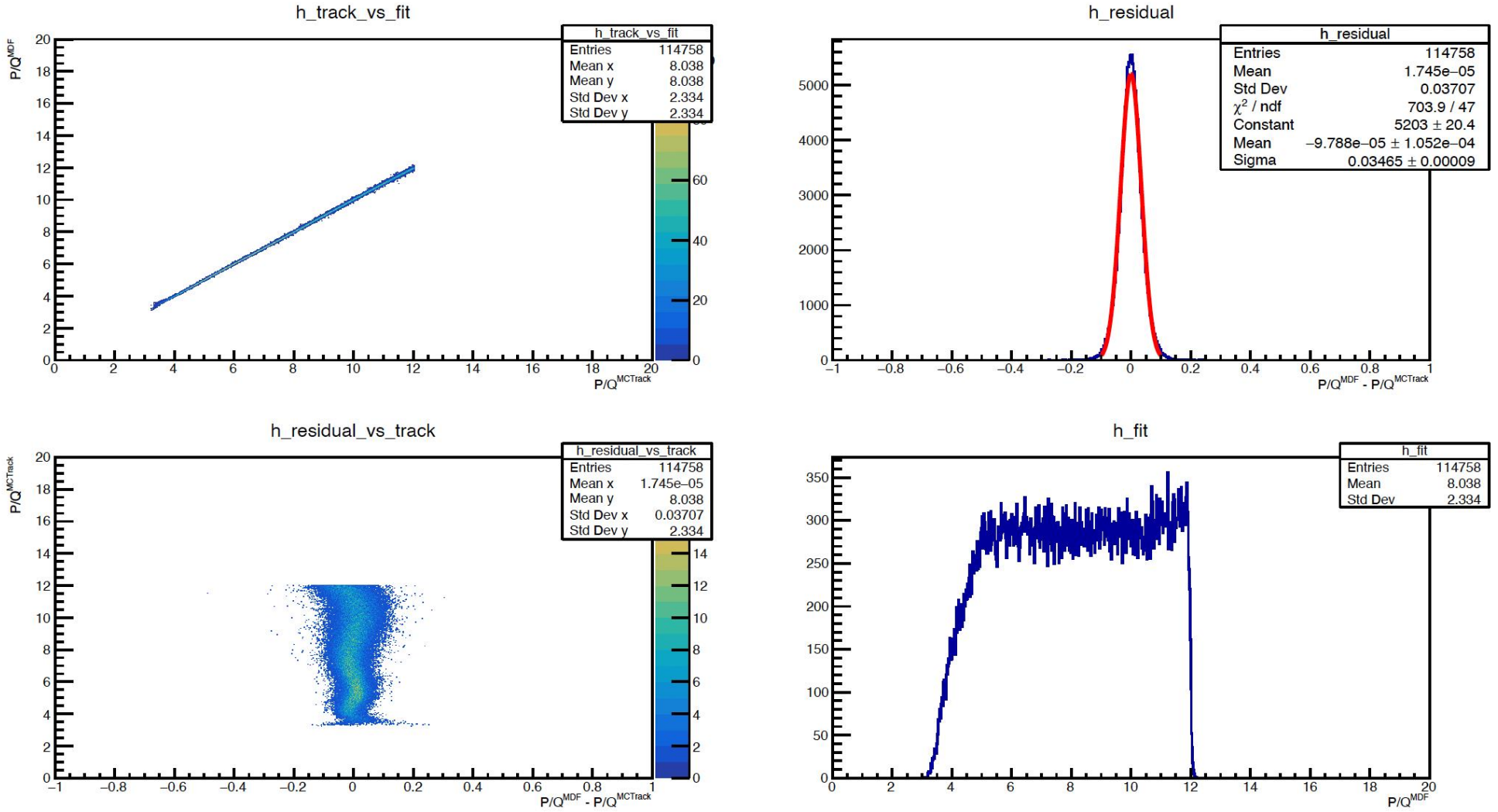

Figure 90: The results of Multi-Dimensional Fit to 300 000 simulated Monte-Carlo tracks of ^{12}C without detector resolutions. P/Q_{track} is the true value (simulation input) and P/Q_{mdf} is the corresponding value obtained from the Multi-Dimensional Fit.

Heavy-fragment identification

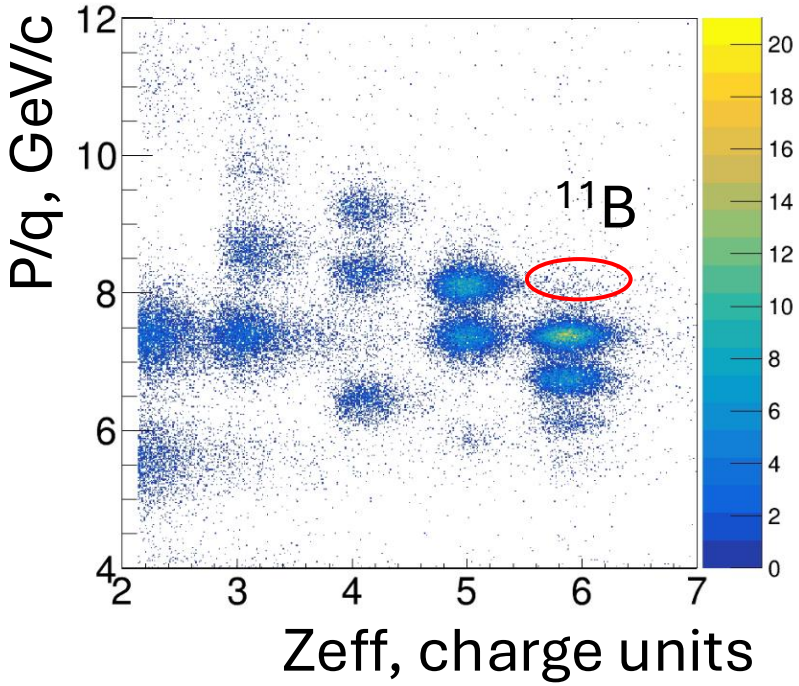

Fragment identification

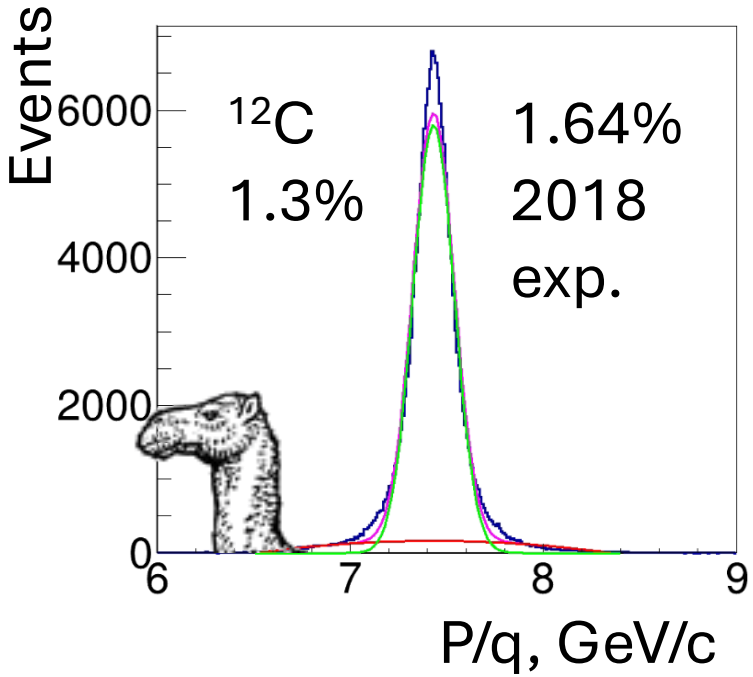

Beam momentum resolution

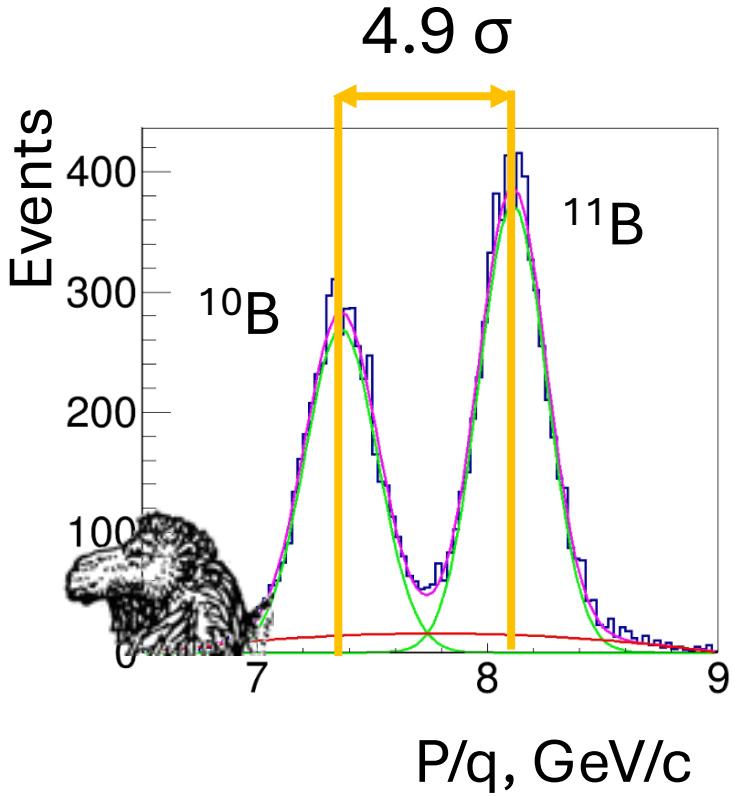

Boron isotopes separation

Total fragment-tracking efficiency

Including the detection efficiency of the MWPC-Si tracks, DCH tracks, track reconstruction, selection, identification algorithms

7.6. Tracking efficiency

Table 35 lists the main contributions to the extracted efficiency (without QE cut). The efficiency drop to 44% is due to matching cuts (ΔTx, ΔTy) we applying to reconstruct P/q.

Table 17: Efficiency of global tracking for single track events.

Condition	N events / Efficiency
Initial number of events	131.7 %
$Z_{in} = 6, Z_{out} = 6$	100 %
Upstream track	82.9 %
DCH track	85.1%
Upstream track and DCH track	70.6 %
P/q^{MDF} reconstructed	42.8 %
$^{11}C + {}^{12}C$ identified	0.5% + 40.0% = 40.5%

Quasi-free **(p,2p)** scattering in inverse kinematics

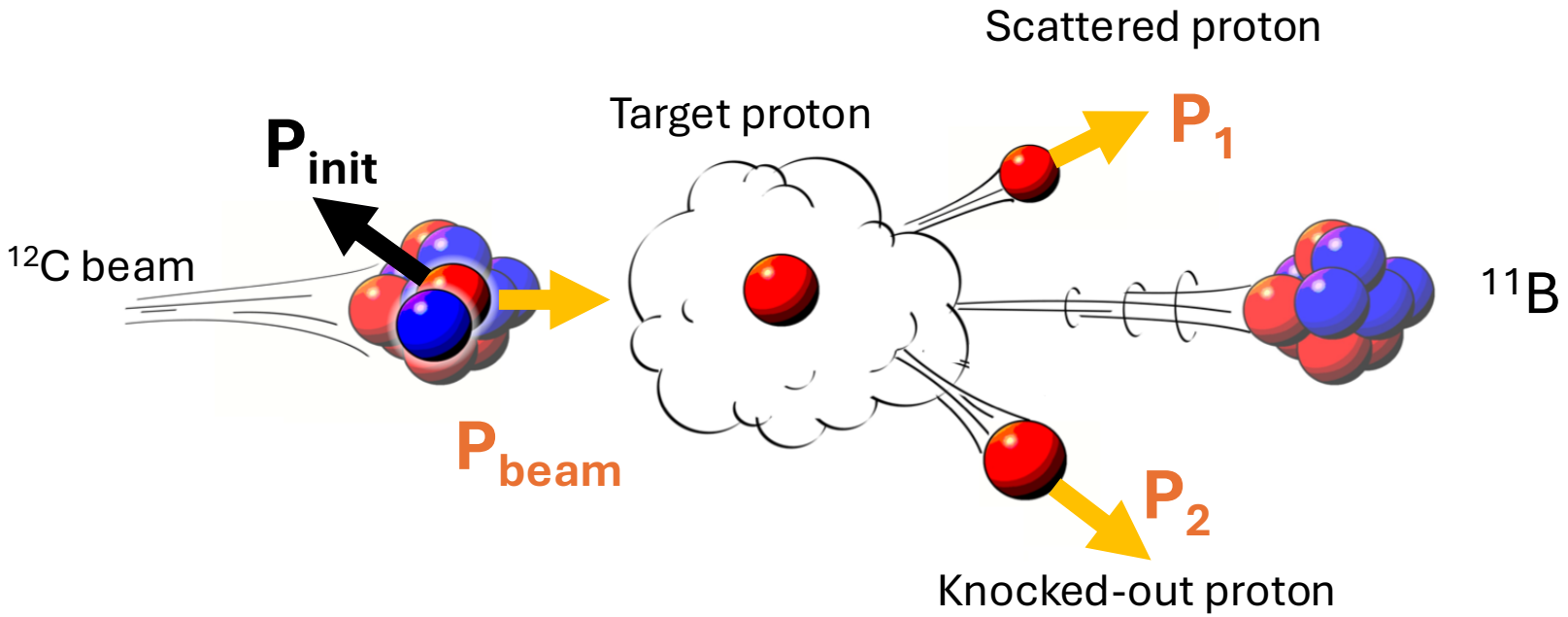

Reconstruct initial nucleon momentum $\mathbf{P_{miss}}$ from scattered particles

with no ISI/FSI $\mathbf{P_{miss}} = \mathbf{P_{init}}$

$\mathbf{P_{miss}} = P_1 + P_2 - P_{beam}$ $\quad M_{miss} = \sqrt{P_{miss}^2}$ $\quad \overrightarrow{p_{miss}} = -\overrightarrow{p_{11B}}$

Arm tracking

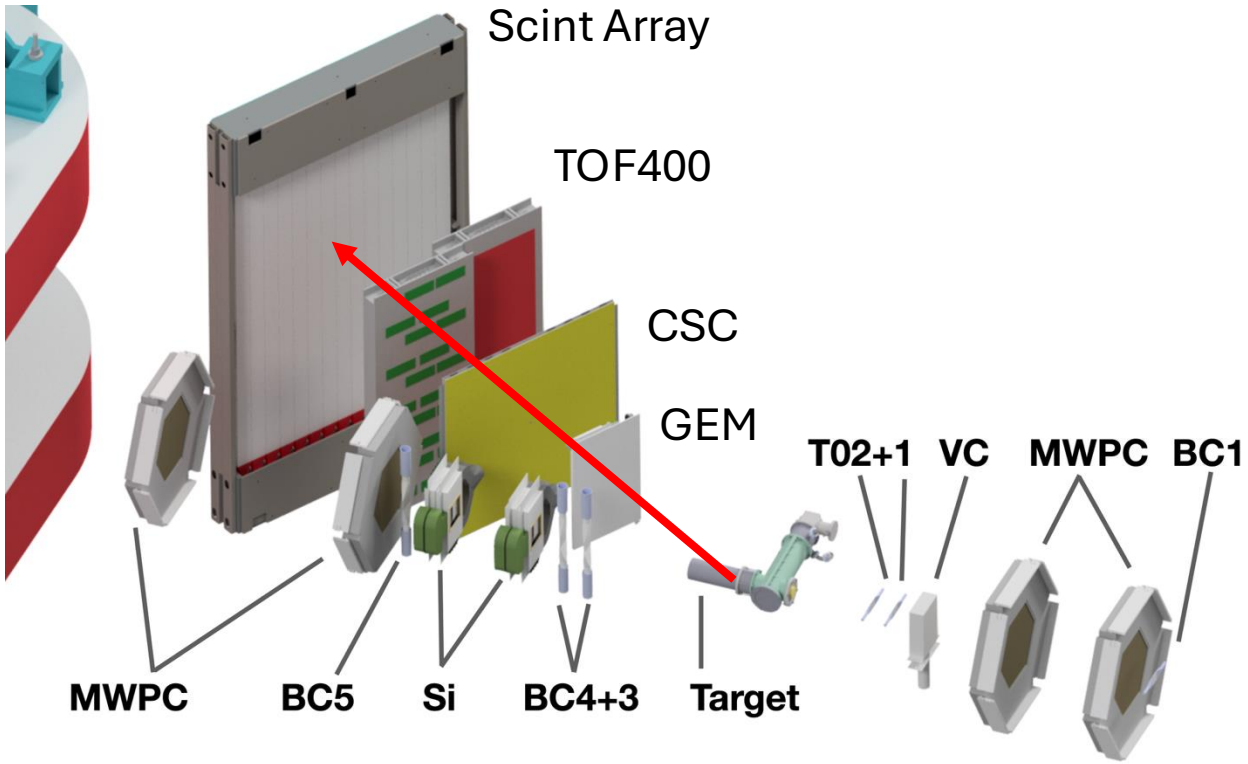

Tracks were done using CSC and TOF400 detectors via Tx and Ty matching within 0.1 rad

Events with more than 1 track in one arm are rejected

Single lead target runs used for calibration: CSC was aligned by minimizing track residuals

Track angular resolution: 4.9 mrad in X and 7.3 mrad in Y

The CSC efficiency is (0.966 +- 0.006) %, TOF400 efficiency is (0.97 +- 0.008) %

Efficiency correction of (12.4 +- 2) % is applied to QE counting

Additional correction of 0.5 % was applied accounting for cases where multi-tracks were identified as single tracks and vice versa.

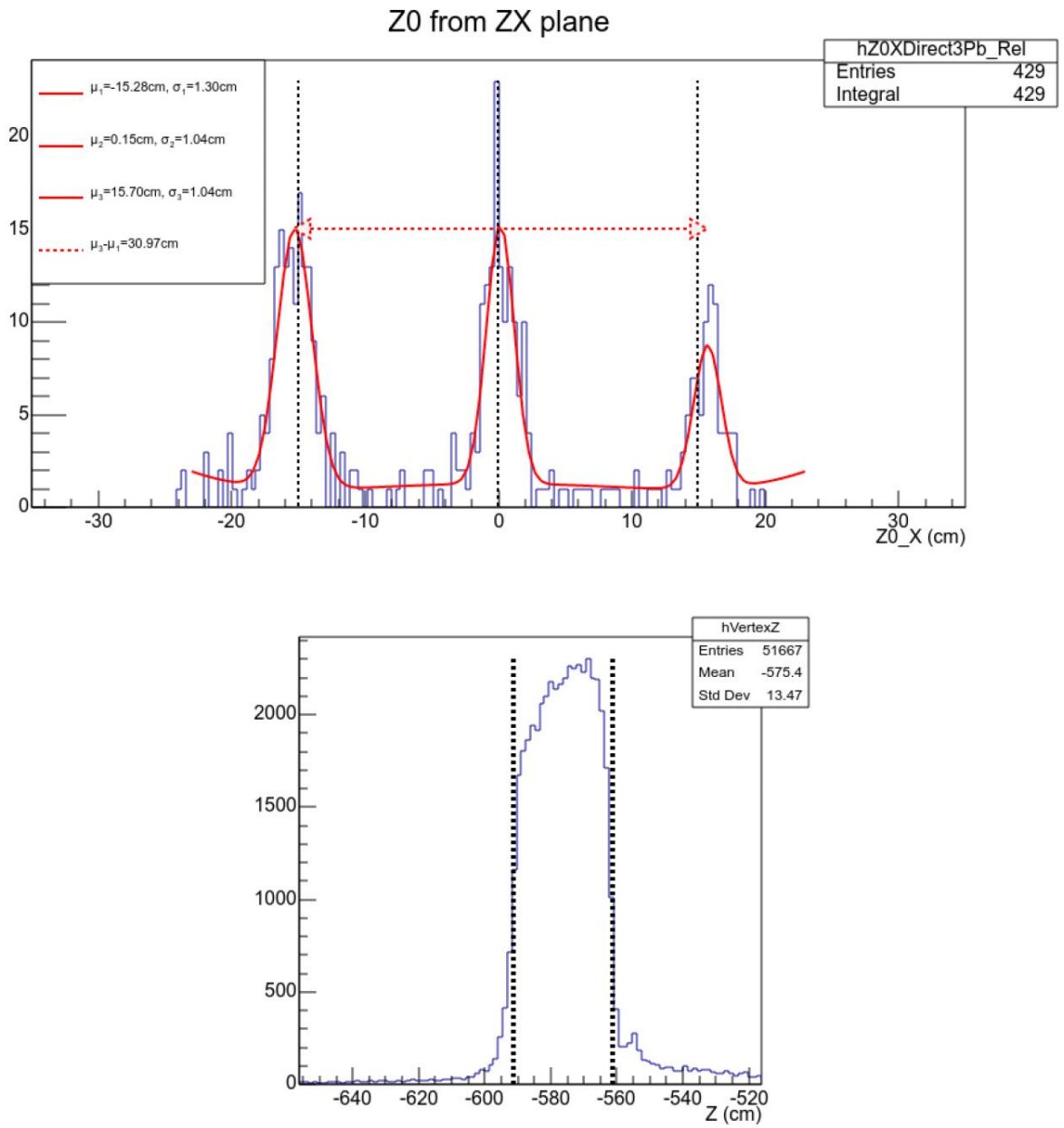

Figure 72: Upper plot: Vertex reconstruction in Z axis for 3 thin lead targets using Gem-Csc combination in both arms. Dashed lines mark the lead targets positions. The red line is a fit of three gaussians and polynomial background. Bottom plot: Vertex reconstruction in Z axis for physics LH2 target. Boundaries of target vessel are marked with black dashed lines.

Z vertex resolution is 2.5 cm

Vertex X, Y were taken from Upstream tracks

ToF in the arms and proton identification

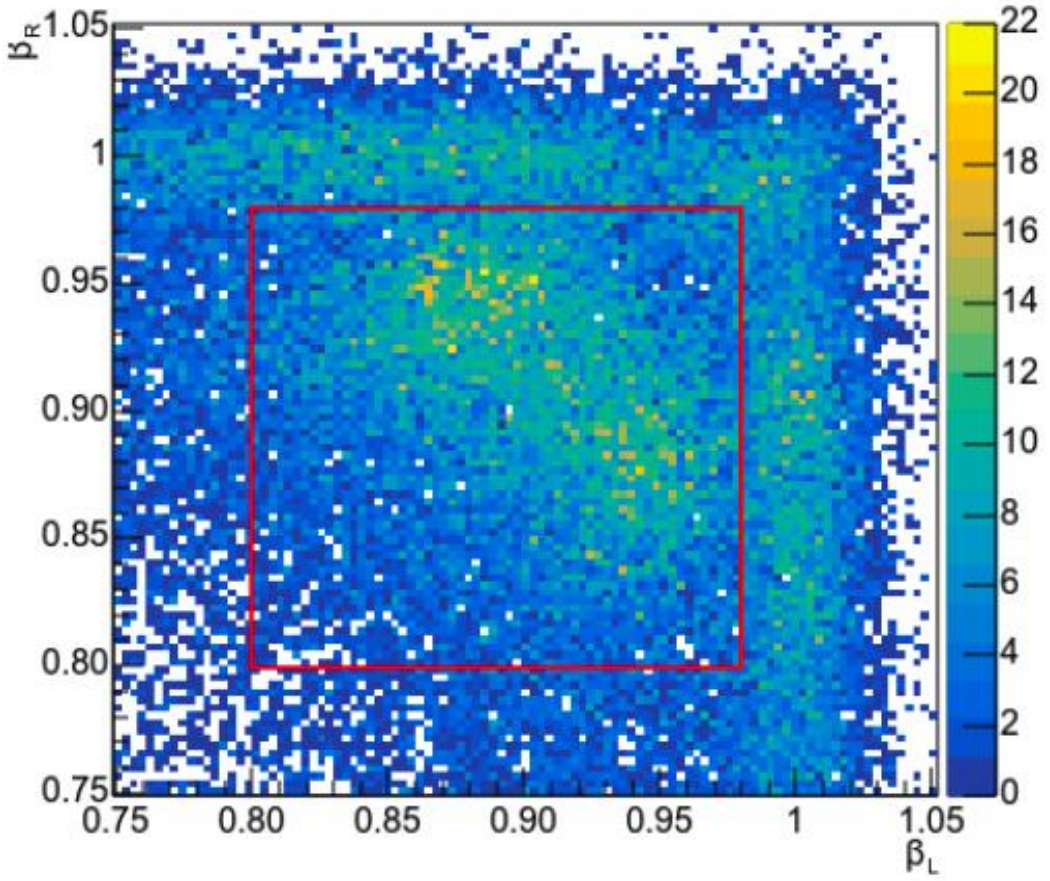

ToF resolution is 170 ps

The total momentum resolution is 150 MeV/c →
Pmiss resolution of 55 MeV/c
The resolution is extracted for QE events in comparison to simulation

Quasi-Elastic identification $^{12}C(p,2p)^{11}B$

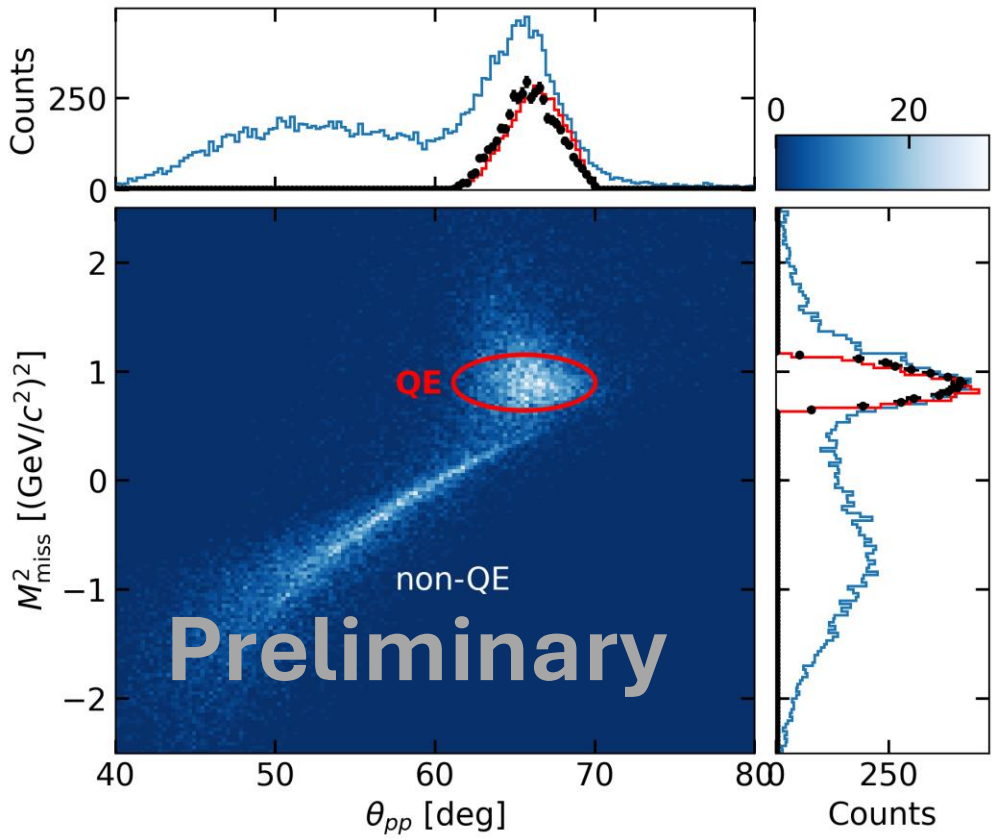

Two single tracks in the arms, 11B, incoming 12C
Reaction vertex within the target
Velocity cut
2d Mmiss2 vs. angle between protons cut

1% uncertainty was estimated as leakage of non-QE events in the red ellipse
Total bkg estimation (2.5 +-2.2) %

Missing momentum $P_{miss} = P_1 + P_2 - P_{beam}$

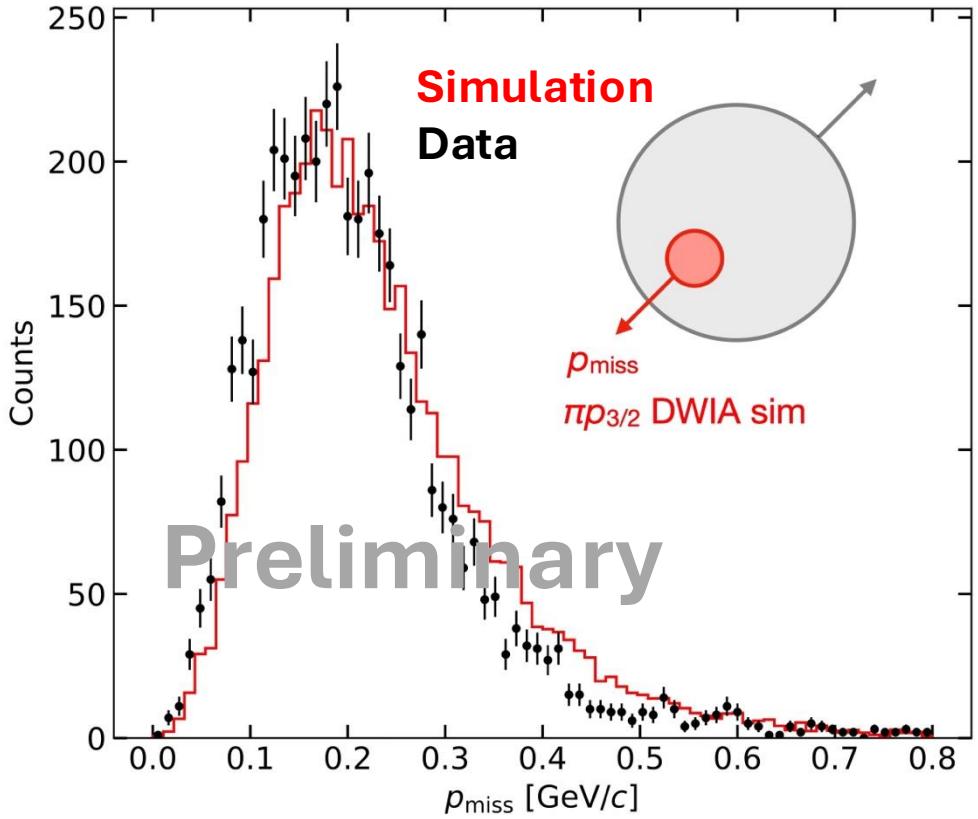

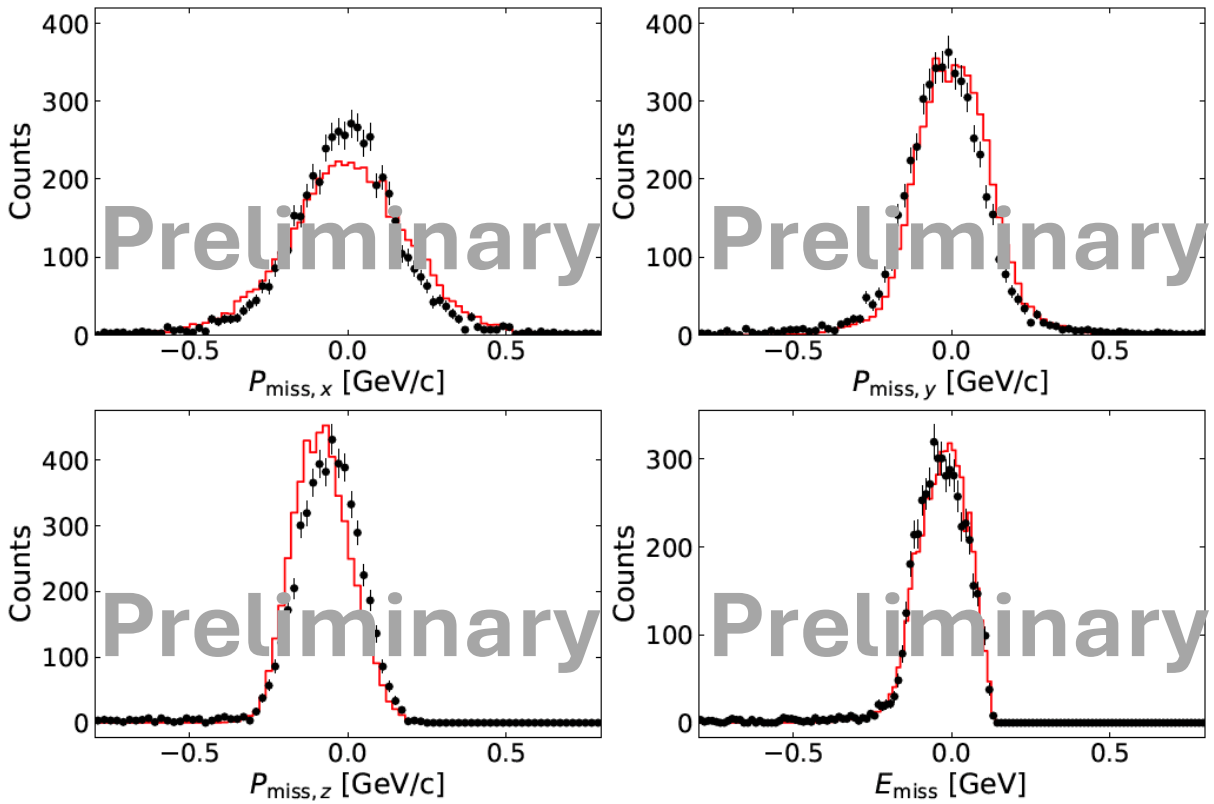

Pmiss resolution is 55 MeV/c approximated by a Gaussian shape, as extracted for QE events from simulation

Mandelstam t, u

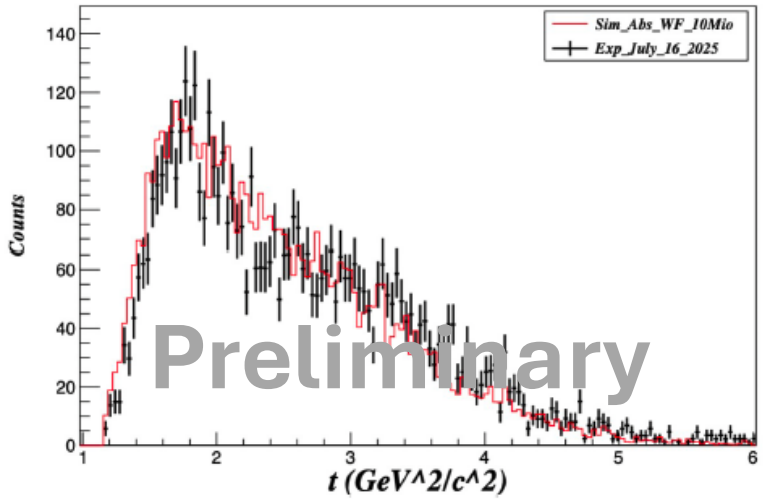

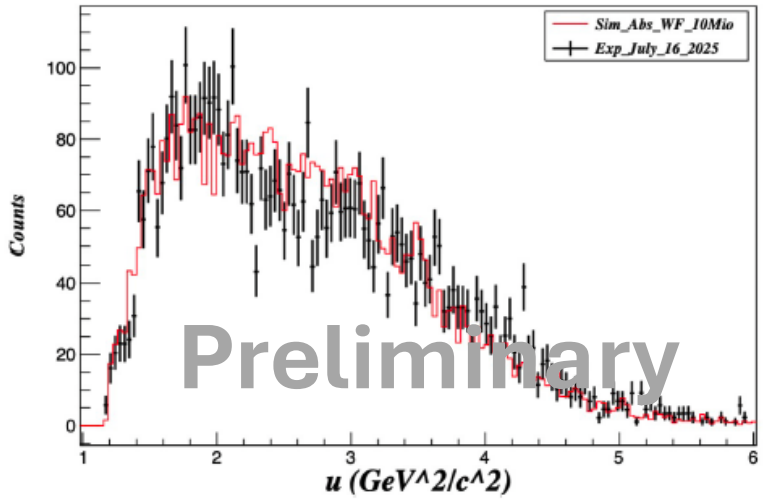

Agreement btw simulation and data (area-normalized) shows

- rejection of non-QE events is ok
- validates the resolutions and acceptance (geometrical and kinematical)
- illustrates that the simulation has a good control over ISI/FSI

Protons in the arms

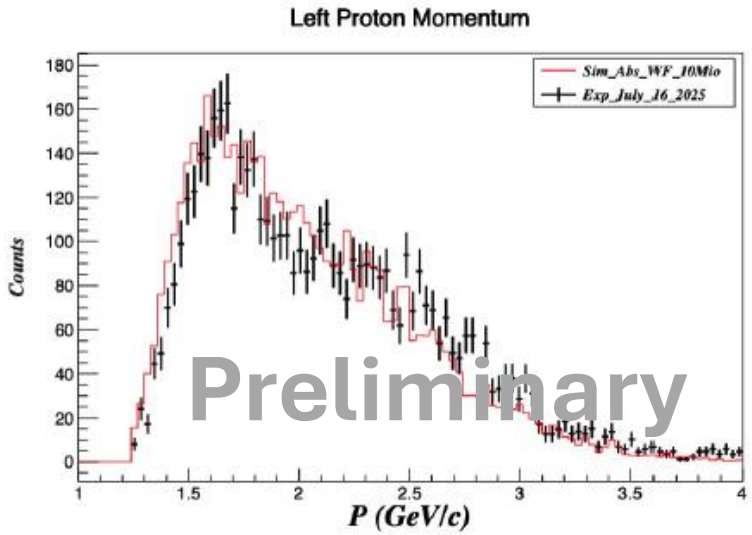

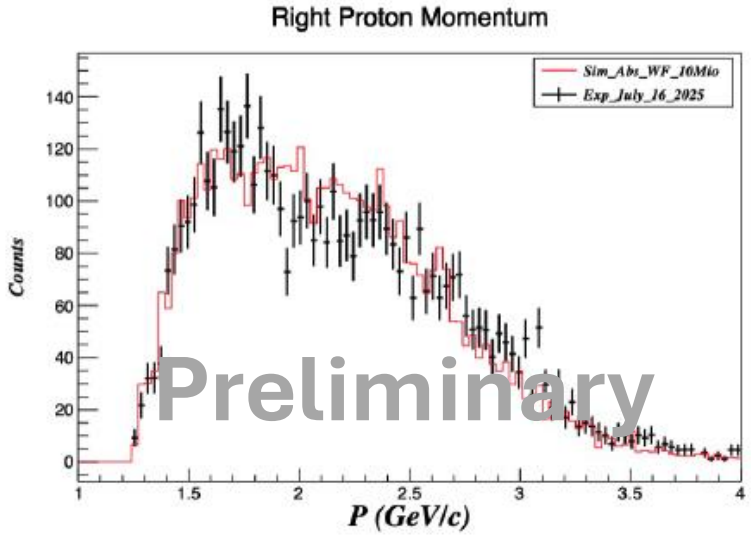

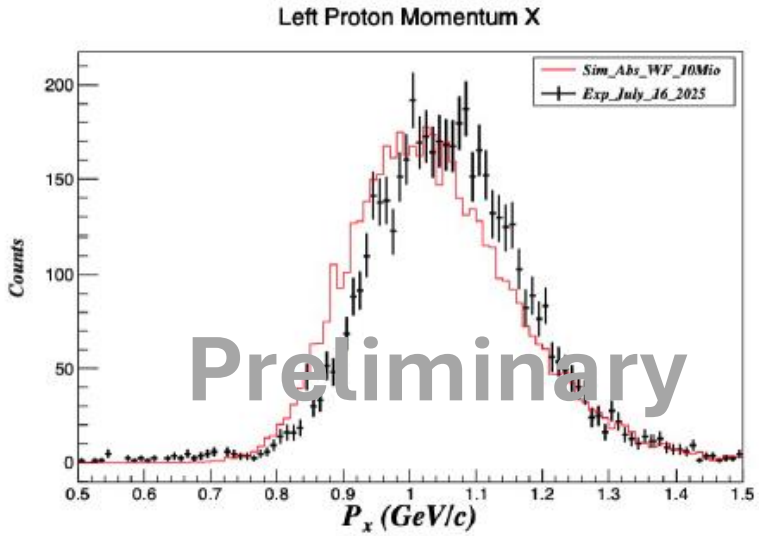

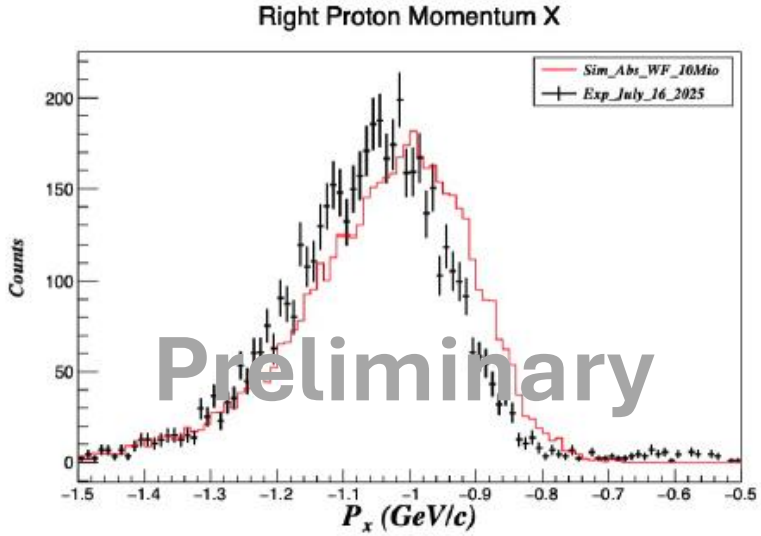

Protons in the arms

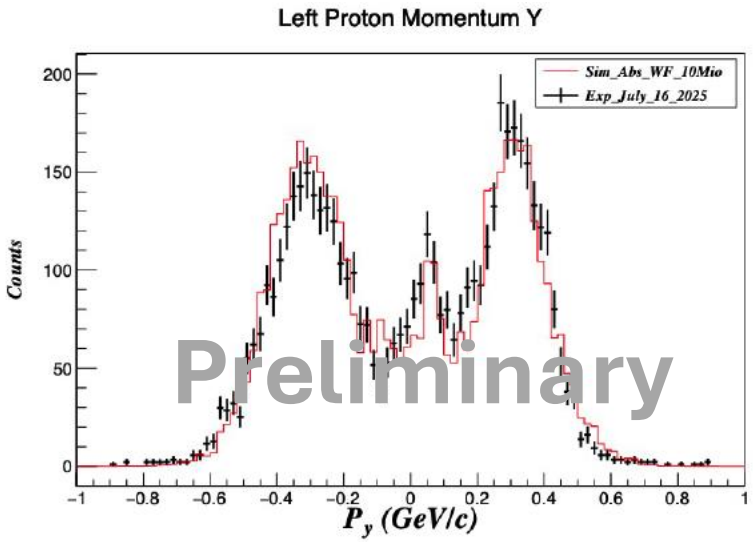

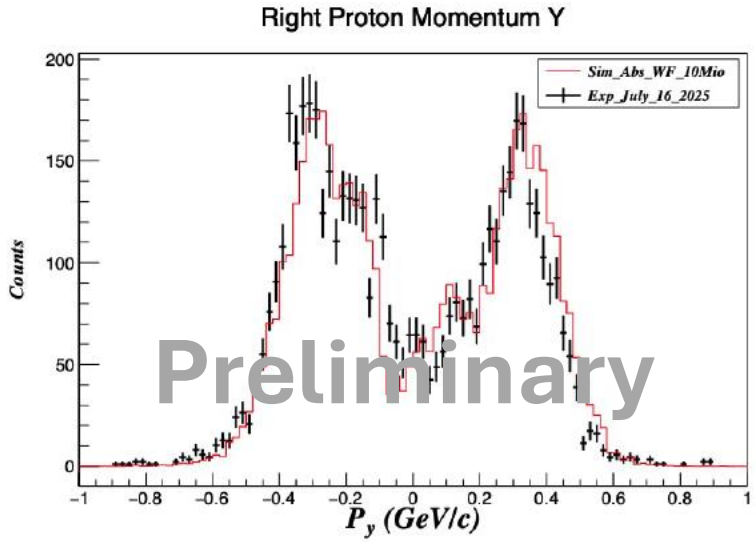

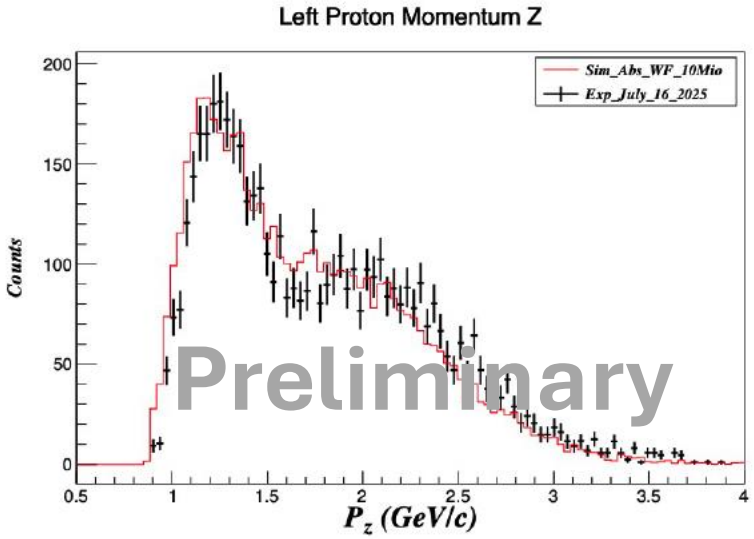

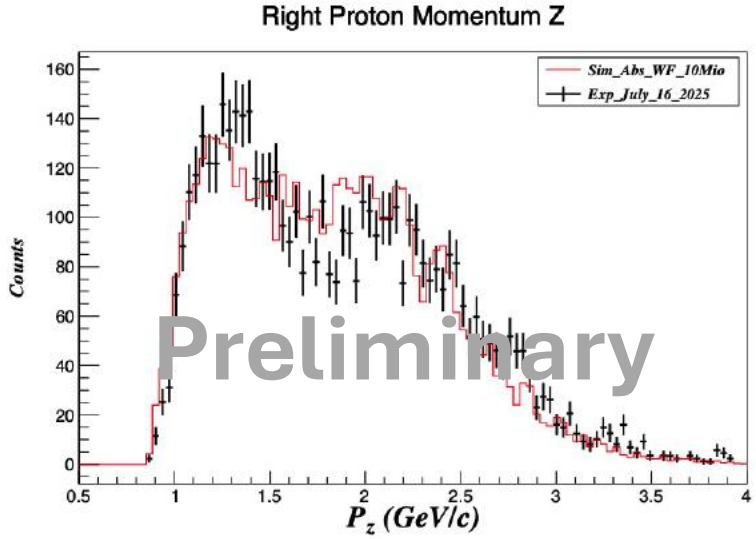

^{11}B momentum

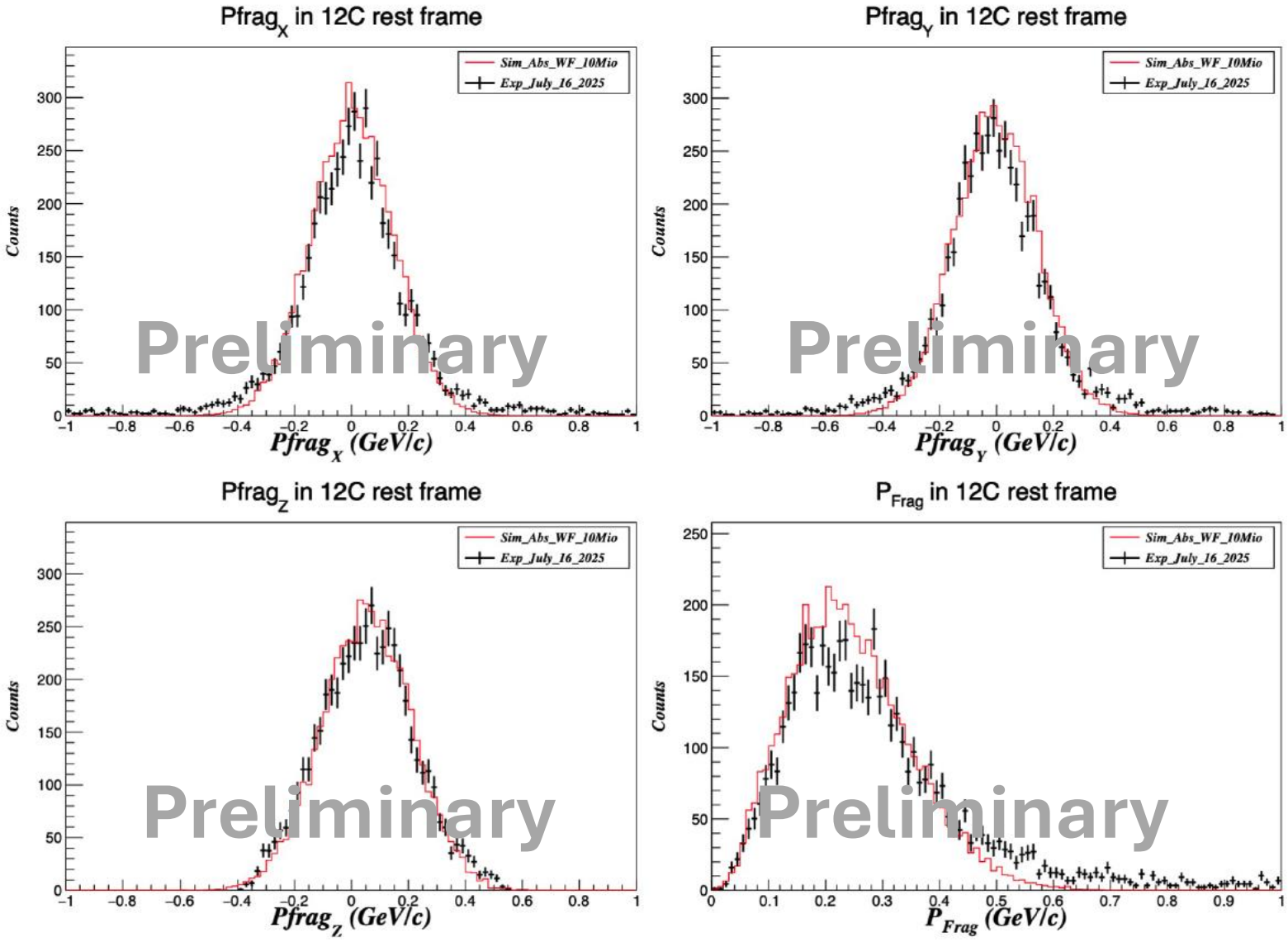

QE cross section

$$\sigma_{QEp} = \frac{N_{(p,2p)11B}(T)}{N_{12C}} \frac{1}{T} \cdot e^{\sigma_R T}$$

T – number of protons in the target ($\sim \rho L$)
σ_R- reaction cross section

Corrections:

Beam-trigger corrections

Fragment
- tracking efficiency
- P/Z cut and background
- Z cut

(p,2p)
- Detector and tracking efficiency
- QE false positive
- MRPC acceptance

Cross section corrections

TABLE II. Correction factors to experimental QE event number N_{reac} for cross-section calculation and relative uncertainties.

Correction	Value	rel. Uncertainty
Downscaling	685	-
Beam trigger correction	0.982	-
QE $(p, 2p)$ tracking	1.130	2.3%
Non-QE background	0.975	2.3%
Fragment P/Q cut	1.036	-
Fragment P/Q background	0.965	1.0%
Fragment Z cut	1.048	-
Fragment reconstruction efficiency	2.522	2.5%
Target (scattering centers)		0.5%
Cut variations		1.8%
$(p, 2p)$ detector acceptance	1.527	1.0%
$(p, 2p)$ ϕ acceptance	7.273	-

Downscaling is obtained by counting how many ArmAnd come with and w/o BT
Nominal downscaling is 700

Fraction of GoodBeam triggers relative to Beam triggers from MSC1

Cross-section systematic uncertainty was obtained using cut sensitivity study. Cut variations include reaction vertex Z, proton angles, velocities, Mmiss, c.m. scattering angle, momentum transfer.
Together they contribute 1.8 % uncertainty compared to the theory expectations

The cross-section stability over the data taking period was checked

Cross-section benchmarking

Interaction cross section: $^{12}C \rightarrow X$

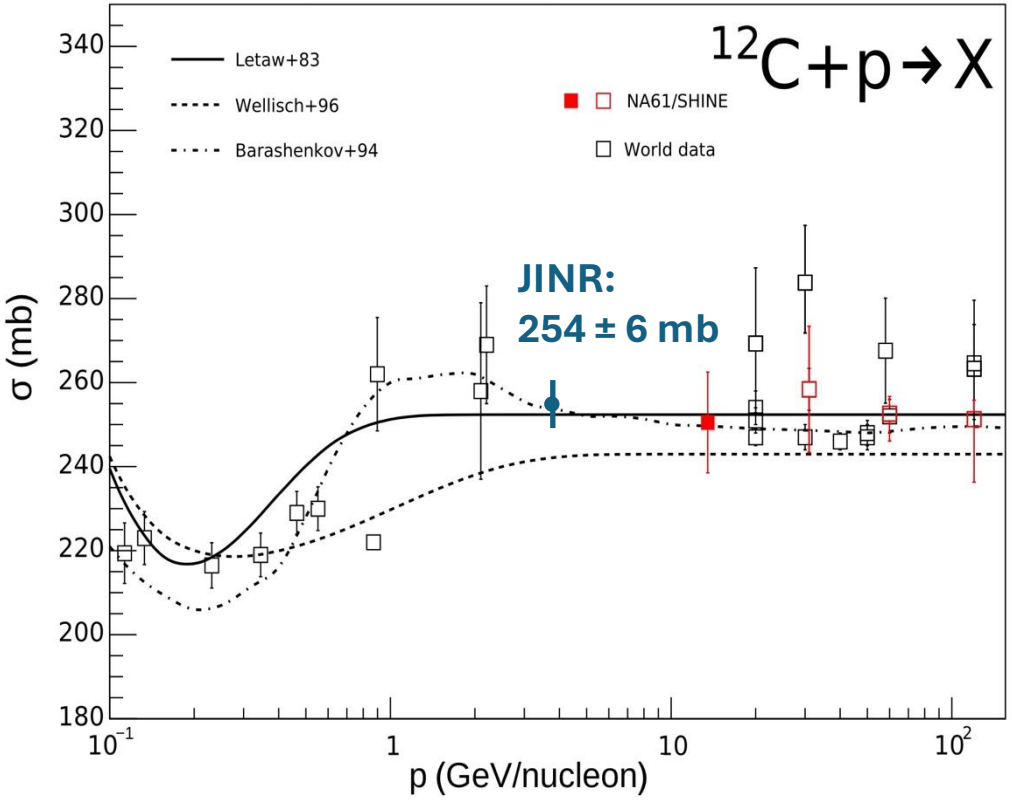

A. Korejwo et al., J. Phys. G 26, 1171 (2000)

Cross-section benchmarking

Interaction cross section: $^{12}C \rightarrow X$

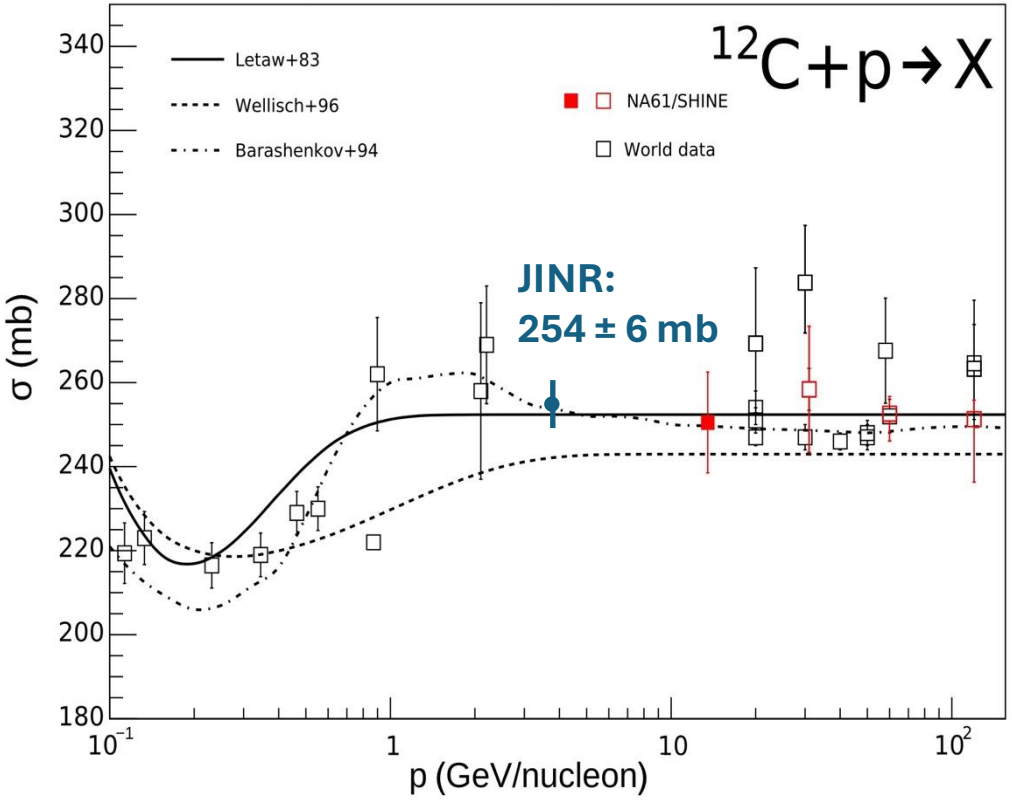

Reaction cross section: $^{12}C \rightarrow {}^{11}B$

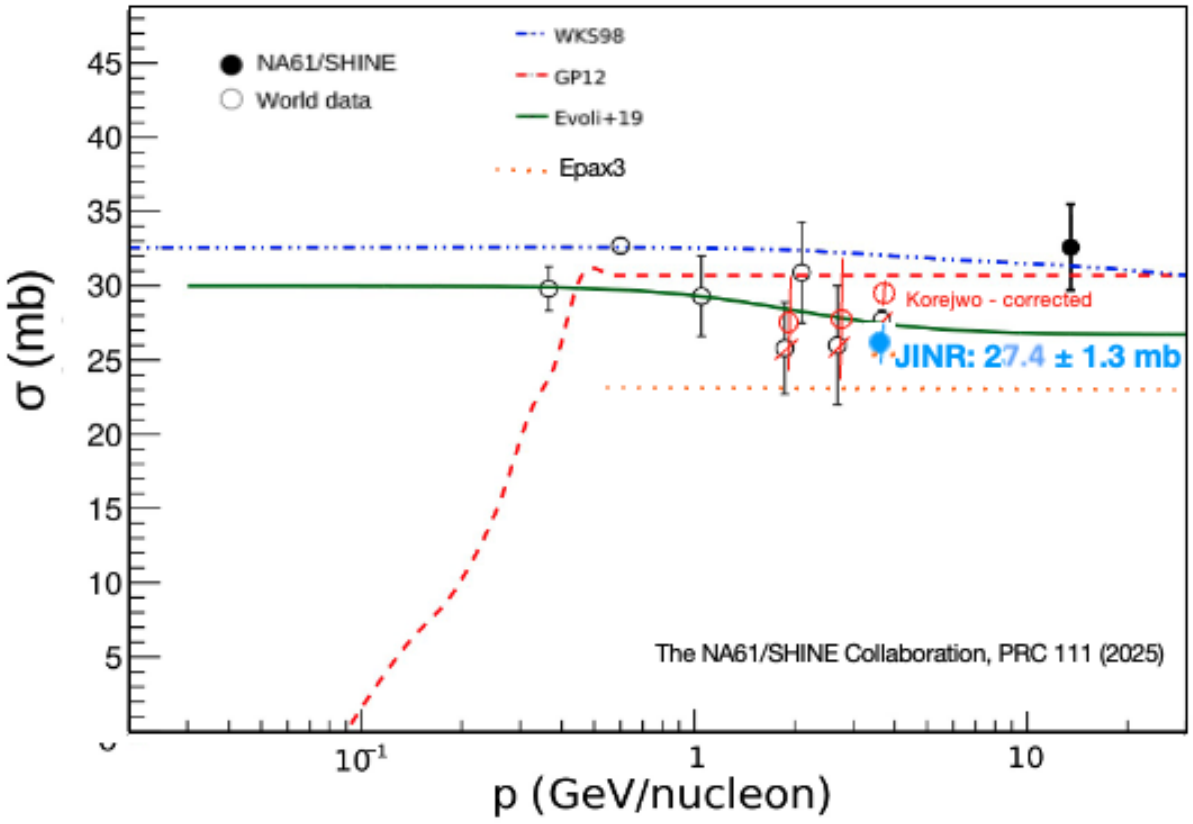

H. Adhikary et al. (NA61/SHINE), Phys. Rev. C 111 (2025)

A. Korejwo et al., J. Phys. G 28 1199 (2002)

QE cross-section $^{12}C(p,2p)^{11}B$

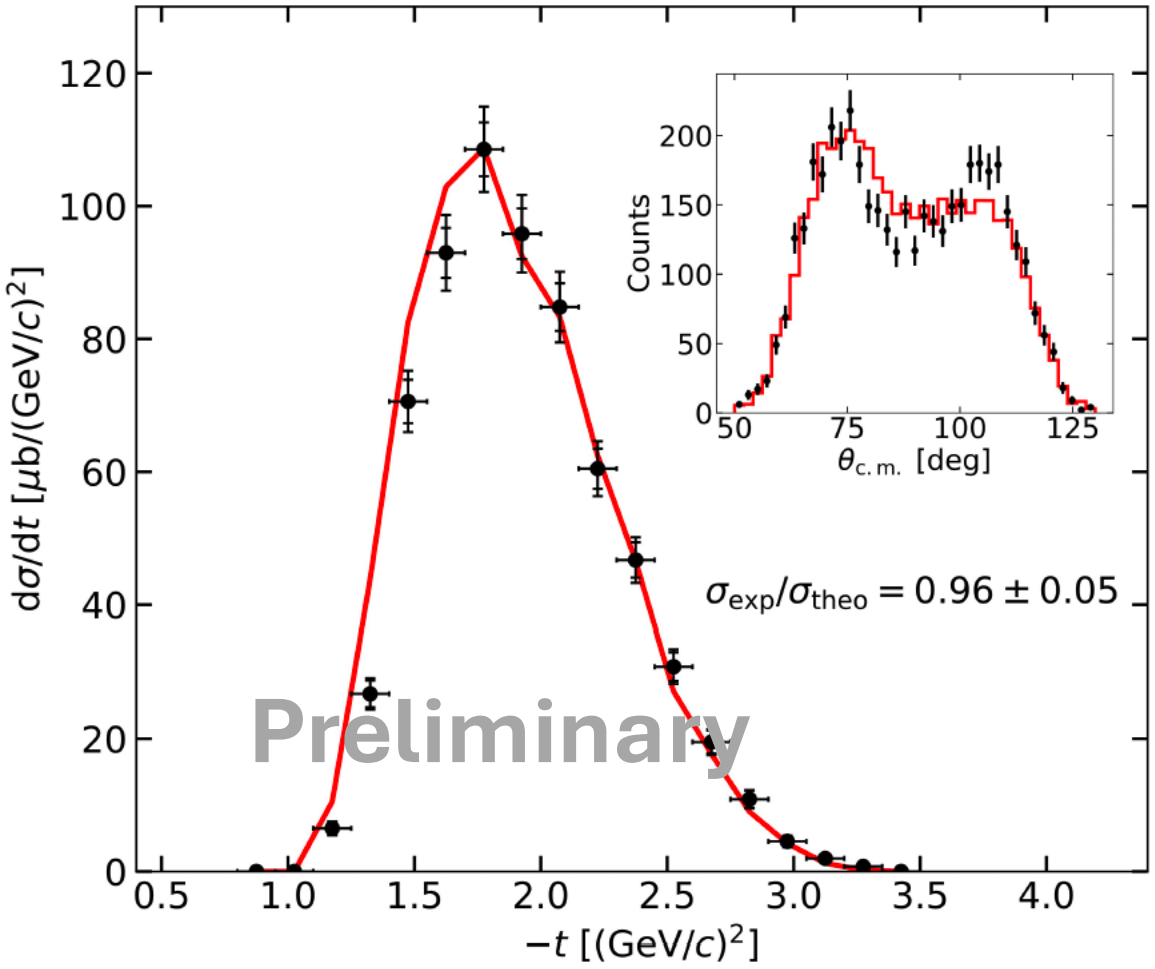

pp-scattering:

$t = (P_1 - P_3)^2 = (P_2 - P_4)^2$

$u = (P_1 - P_4)^2 = (P_2 - P_3)^2$

QE (p,2p) process at intermediate relativistic energies

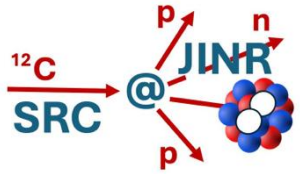

Theory by Alexey Larionov and Yuri Uzikov, PRC 110 (2024)

Nuclear Structure	**x**	**(p,2p)**	**x**	**ISI/FSI**
Translationally invariant shell model (here: HO WF)		Impulse Approximation		Glauber Calculation

Nuclear Structure x **(p,2p)** x **ISI/FSI**

Translationally invariant shell model (here: HO WF)

Impulse Approximation

Glauber Calculation

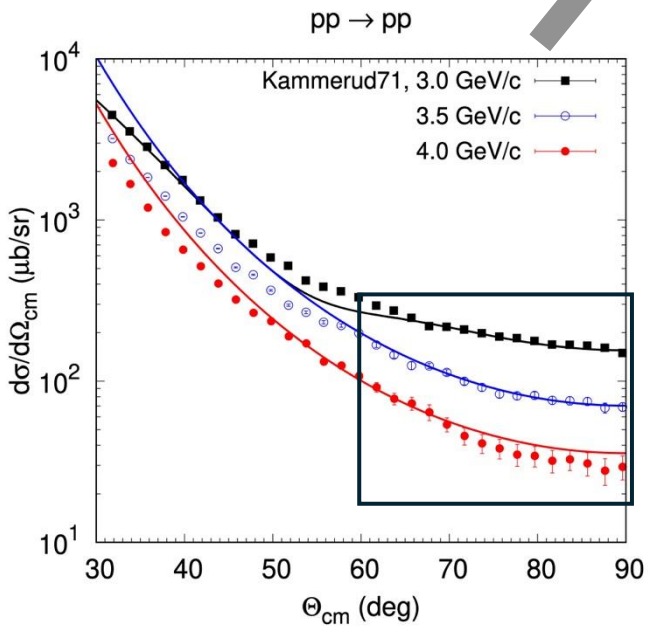

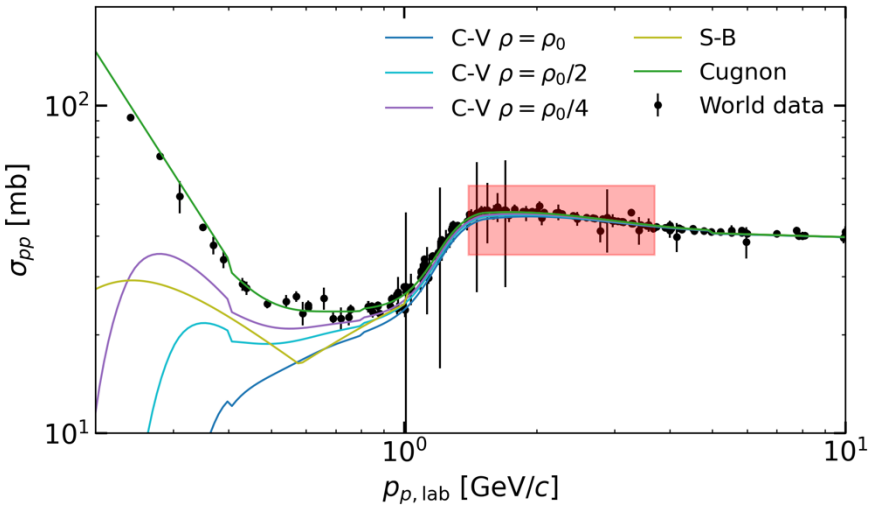

data - L. R. Workman et al. (Particle Data Group), PTEP 2022, 083C01 (2022)
J. Cugnon et al., Nucl. Instr. Meth. B 111, 215 (1996)
R. D. Smith and M. Bozoian, Phys. Rev. C 39 1751 (1989)
E. Clementel and C. Villi, Il Nuovo Climento 2, 176-179 (1955)

QE cross-section $^{12}C(p,2p)^{11}B$

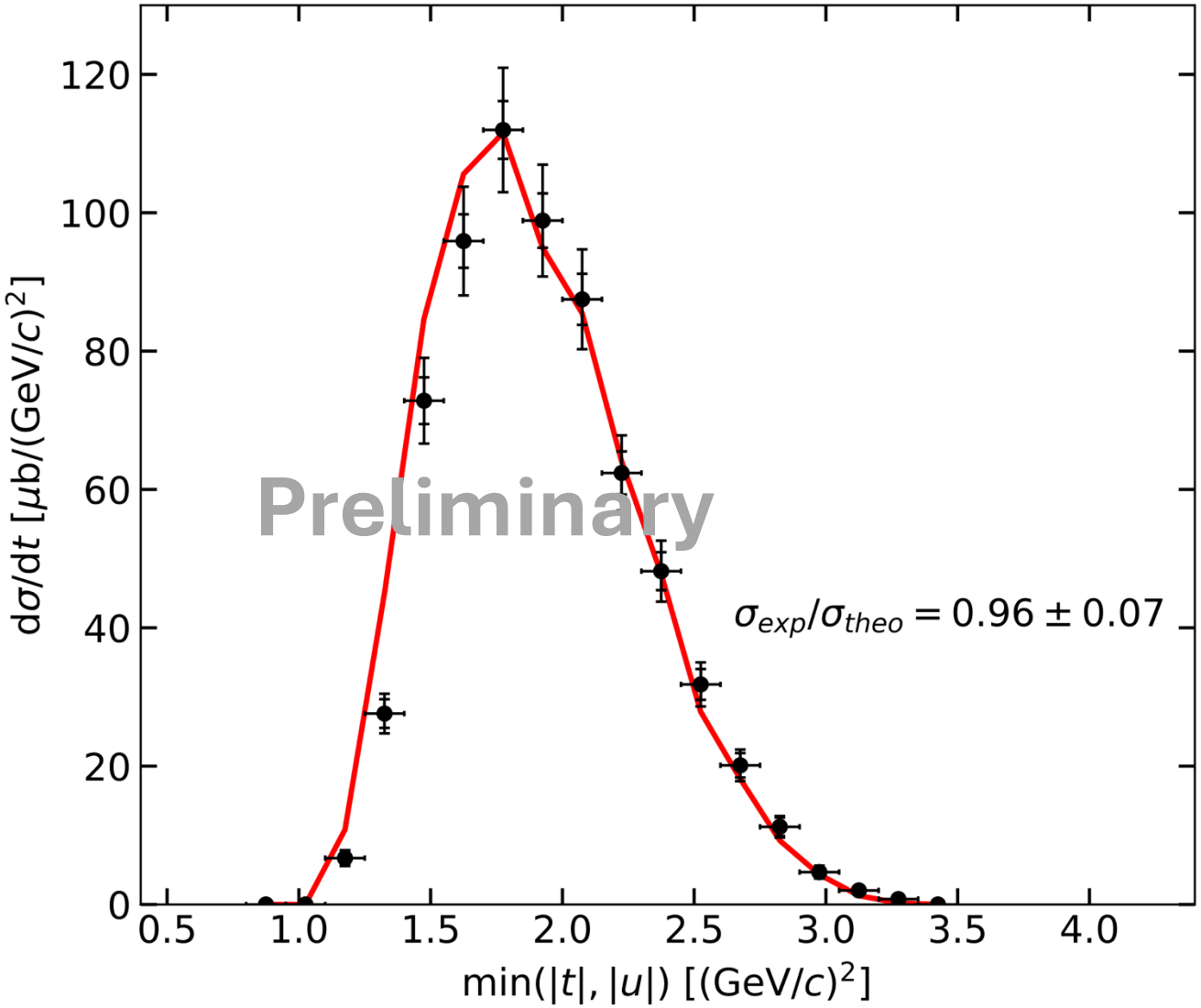

pp-scattering:

$t = (P_1 - P_3)^2 = (P_2 - P_4)^2$

$u = (P_1 - P_4)^2 = (P_2 - P_3)^2$

$$R_s = \frac{\sigma_{exp}}{\sigma_{theory}} = 0.96 \pm 0.07$$

^{12}C spectroscopic strength: scale dependence

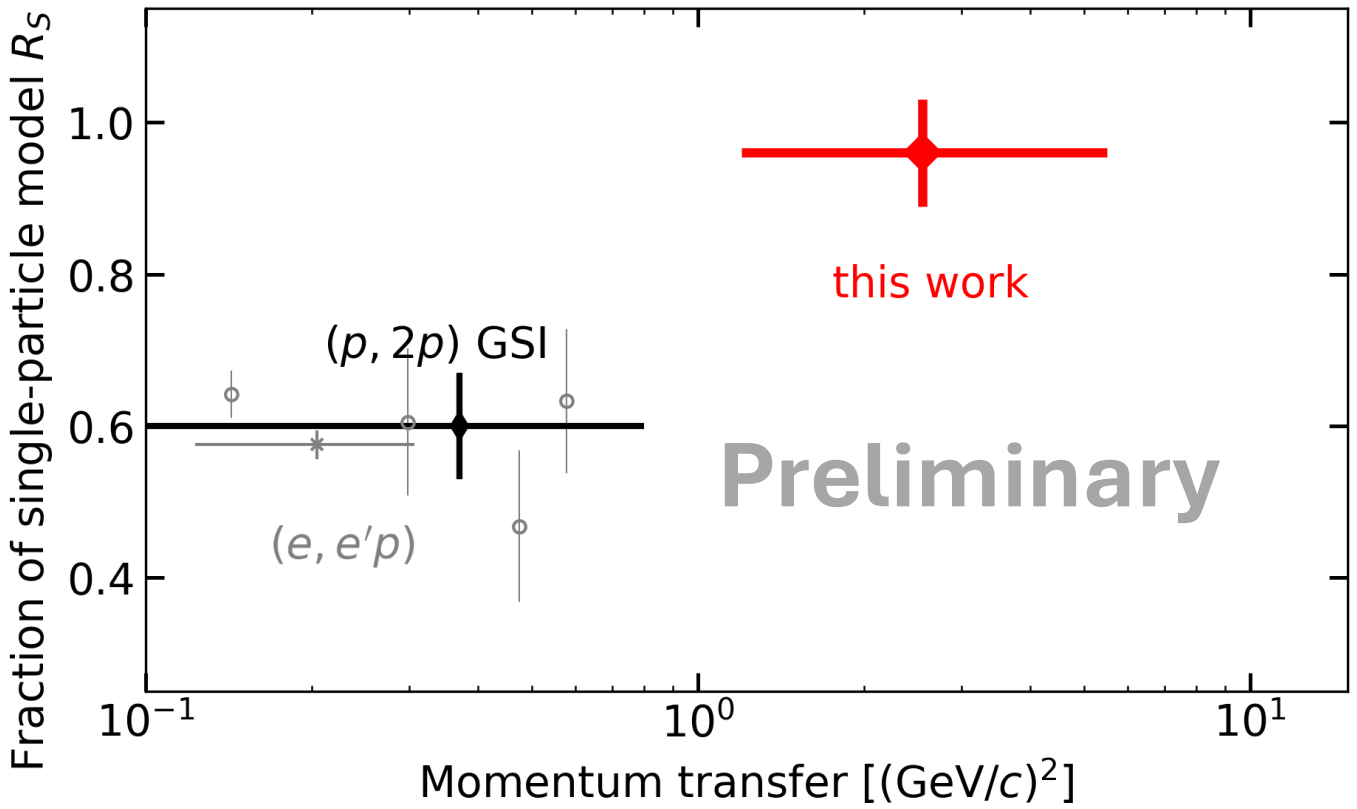

^{12}C spectroscopic strength: scale dependence

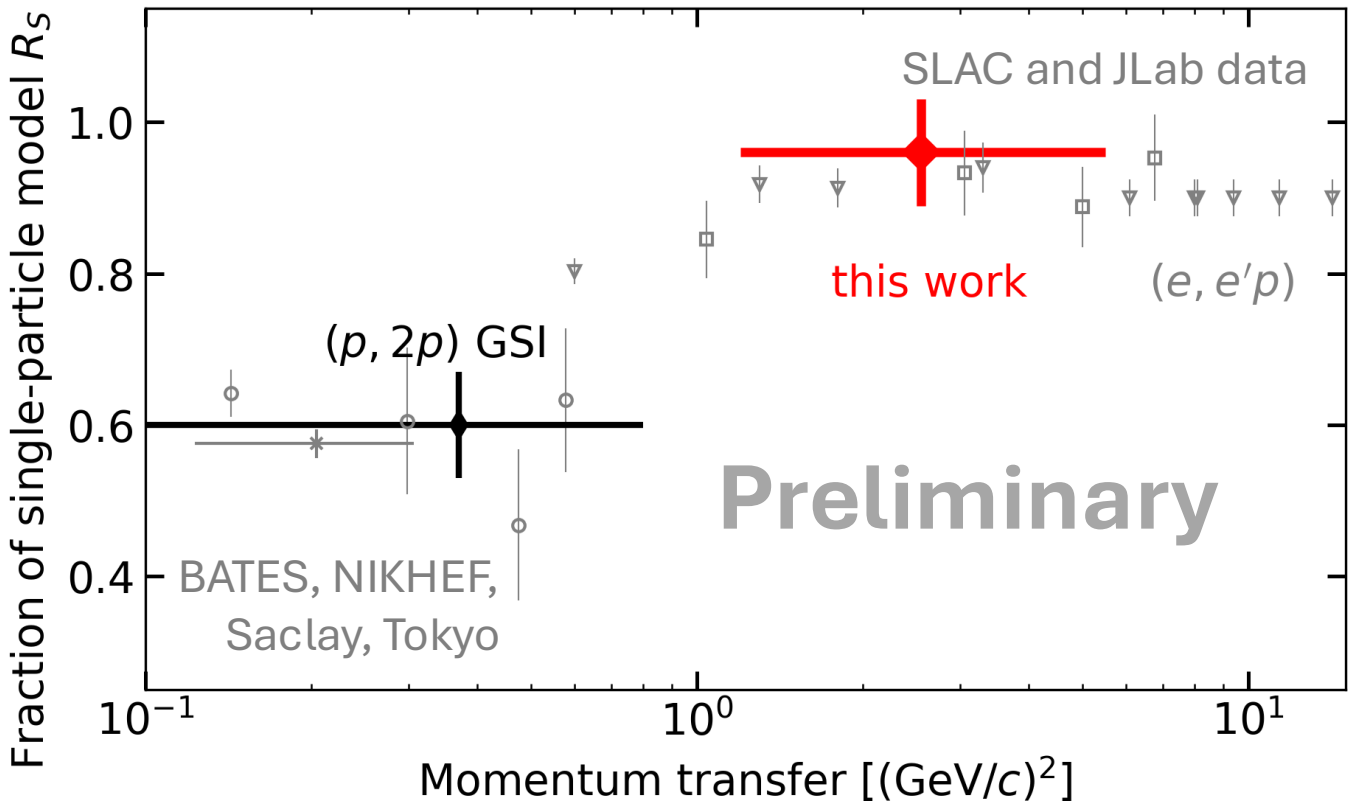

L. Lapikas et al., Phys. Rev. C 61, 064325 (2000)
D. Bhetuwal et al. (Hall C), Phys. Rev. Lett. 126, 082301 (2021)
N. Makins et al., Phys. Rev. Lett. 72,1986 (1994)
D. Abbott et al., Phys. Rev. Lett. 80, 5072 (1998)
P. E. Ulmer et al., Phys. Rev. Lett. 59, 2259 (1987)
L. B. Weinstein et al., Phys. Rev. Lett. 64, 1646 (1990)
K. Garrow et al., Phys. Rev. C 66, 044613 (2002)
V. Panin et al., Phys. Lett. B 753, 204 (2016)

Summary

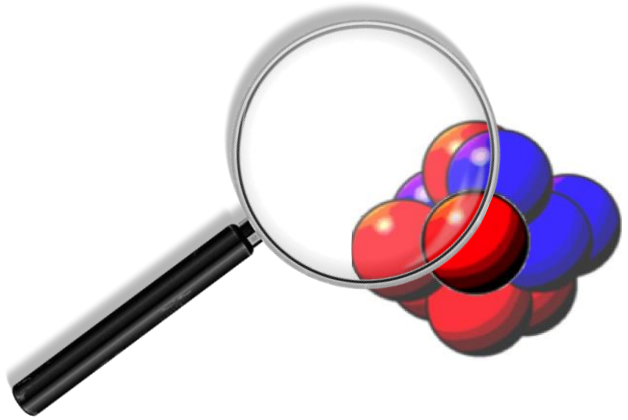

^{12}C spectroscopic strength is scale dependent

"Unquenching" → Universal, resolution-dependent restoration of the single-particle picture

Favorable kinematics:

- High energy → ISI/FSI in Glauber approach
- High momentum → resolution scale

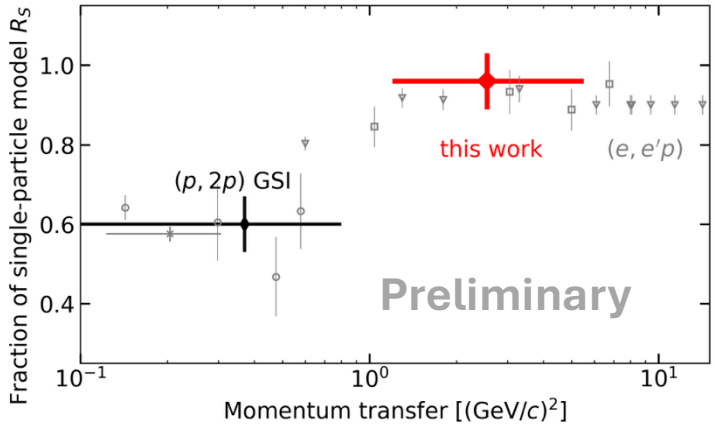

Thank you!

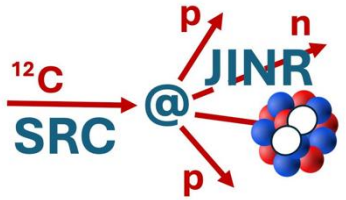

International SRC at JINR group

Students

